

# Building demolition estimation in urban road widening projects using as-is BIM models

Feng Jiang<sup>a</sup>, Ling Ma<sup>a,\*</sup>, Tim Broyd<sup>a</sup>, Ke Chen<sup>b</sup>, Hanbin Luo<sup>b</sup>, Muzi Du<sup>c</sup>

<sup>a</sup> The Bartlett School of Sustainable Construction, University College London, London WC1E 6BT, UK

<sup>b</sup> School of Civil and Hydraulic Engineering, Huazhong University of Science and Technology, Wuhan 430074, China

<sup>c</sup> CCCC Water Transportation Consultants Co., Ltd., Beijing 100007, China

## ARTICLE INFO

### Keywords:

As-is BIM  
Building information modelling (BIM)  
Road widening  
Road engineering  
Alignment fitting  
Building demolition  
Cost estimation

## ABSTRACT

Building demolition caused by urban road widening projects can lead to engineering, economic, and environmental issues and should be planned at the design stage. Based on as-is BIM, this paper proposes a method to estimate the building demolition caused by urban road widening using online map data and statistics on government websites. The as-is BIM models of the existing old road and its surrounding buildings are created, and the BIM models of the newly widened road are built based on the as-is BIM models considering road components in accordance with road engineering expressions to assist building demolition estimation using clash detection. This paper presents a cost-effective building demolition estimation in urban road widening projects without field surveys. It was tested on the M4 Motorway project in London. It has been proved to be a very practical approach to facilitate urban road planning and decision making.

## 1. Introduction

Many existing old roads were designed and constructed decades ago, which cannot meet the up-to-date traffic demands from society [37]. Road widening is one of the most common solutions to improve roads' level of service (LOS) [61,63]. In addition to considering benefits brought by road widening, several constraints should be considered, such as engineering factors, construction quantity and costs, impacts on the surroundings, impacts on society, etc. [30]. In the urban built-up areas, building demolition is widely recognised as one of the most significant factors hindering road widening, which can cause many economic, environmental, and democratic issues [3]. There are two methods to estimate building demolition during a road-widening project. First, in the preliminary design phase, designers can simply offset the boundary lines of the existing road outwards by a specific value on the 2D map according to the widened width of the pavement to represent the new boundary lines of the widened road. However, a road is a 3D structure that consists of horizontal alignments, vertical alignments, cross-sections, crossfalls, superelevations, and side slopes [27]. When the pavement of an existing road is widened by a specific value, the new boundary lines of the newly widened road generated by the intersection relation between side slopes and the terrain in the real world can be very

different from the simply offset boundary lines on the 2D map, as shown in Fig. 1. In addition, different buildings have different heights, floor areas, and prices which can cause various demolition costs [15]. In the second method, a detailed field survey and negotiations with property owners can be conducted to estimate the demolition cost during a road-widening project, which is labour-intensive, costly, and time-consuming for the preliminary design. Unlike newly built road projects, road widening should be designed and constructed based on existing old roads. Before new lanes, hard shoulders, verges, embankments and side slopes are constructed, horizontal alignments, vertical alignments, and cross-sections of the existing old roads should be fitted to assist in road widening [22,29]. Thus, for urban road widening design and construction, collecting, recreating and interpreting data of the existing old road and surrounding buildings is essential. However, the old design and construction data and documents of the existing old road and buildings are difficult to find completely. Since these projects did not employ enough digital means during construction in the past, even if some of their data and documents could be found, they are unstructured data, such as 2D PDF or paper drawings, and are challenging to assist in urban road widening and building demolition estimation. Thus, how to digitalise and recreate existing old roads and surrounding buildings should be studied.

\* Corresponding author.

E-mail address: [l.ma@ucl.ac.uk](mailto:l.ma@ucl.ac.uk) (L. Ma).

<https://doi.org/10.1016/j.autcon.2022.104601>

Received 16 June 2022; Received in revised form 16 September 2022; Accepted 27 September 2022

Available online 3 October 2022

0926-5805/© 2022 The Author(s). Published by Elsevier B.V. This is an open access article under the CC BY license (<http://creativecommons.org/licenses/by/4.0/>).

As-is BIM (building information modelling) can provide a feasible solution to this issue. In the design phase of engineering, the as-is BIM model of the existing related projects, surroundings, and environment can be established to assist in decision-making and designing [25,50]. By collecting data from the physical world and parsing data into understandable expressions, as-is BIM model can build digital replicas for existing old roads and surrounding buildings to realise building demolition estimation during road widening. In addition to field surveys, online map data, policy, and government statistics can be employed to estimate the building demolition costs caused by road widening in the preliminary design phase. In addition, BIM can provide 3D models integrating information and non-geometric information to assist simulation, cost estimation, collaboration, decision making, and comprehensive management [5].

This research aims to propose an approach to estimate building demolition during the urban road widening based on as-is BIM of roads and buildings using government statistics, policy, and data from the online map database such as digital surface model (DSM), digital terrain model (DTM), topographies, and aerial photographs without field surveys. The research aim can be divided into several research objectives:

- 1) Develop a systematic workflow based on as-is BIM to estimate building demolition caused by urban road widening.
- 2) Provide a systematic method to build as-is BIM models for roads in accordance with expressions of engineering.
- 3) Propose a method to create as-is BIM models of the buildings along the target road, which can reflect the impacts of the surrounding built environment on existing infrastructure.
- 4) Propose several methods to build BIM models for roads and buildings from online map data and government statistics rather than field surveys.

This paper begins with a systematic review in Section 2. Next, the proposed approach for estimating building demolition will be introduced in detail in Section 3. Then, Section 4 will introduce how the

proposed approach is employed in road widening for M4 motorway in an area called Hounslow in London. Finally, Section 5 is the discussion, and Section 6 is the conclusions of this paper.

## 2. Literature review

### 2.1. Road widening and its impacts on the surrounding

Road widening can alleviate traffic congestion and improve roads' level of service. However, road widening needs to occupy more space and can bring impacts on surroundings. First, road widening can cause building demolition. Pyngrope, et al. [47] studied the potential of demolished building waste caused by road widening as aggregates in alkali-activated concrete. Jiang, et al. [28] proposed a DT (digital twin)-MCDM (multi-criteria decision making)-GIS (geographic information system) framework for sustainable urban road planning using online map data from Digimap and Google Maps, considering road widening and building demolition. Second, road widening should consider the relocation of utility poles and underground pipelines. Husain and Vaishya [23] presented a five-step method to detect pole-like objects along the roadway using three-dimensional terrestrial laser scanner data based on K-means clustering method, ground filtering, and analytical hierarchy process, which can assist the relocation of poles in the road widening projects. Third, road widening can lead to redesigning and reconstructing the existing transportation infrastructure. For example, main road widening can reduce the clearance of the low-level underpass road due to the crossfall and width of the main road and the vertical alignment of the underpass road. Thus, Jiang, et al. [26] proposed a cost-effective approach using online map data to check the clearance of an existing underpass road in a highway widening project based on the digital twin paradigm. Then, the underpass road can be redesigned to ensure the clearance requirement. Fourth, road widening can bring some environmental issues. Phogat, et al. [46] studied the impacts of road widening on the environment, including temperature, deforestation, rainfall, landslides, blasting, surface and groundwater, air and soil

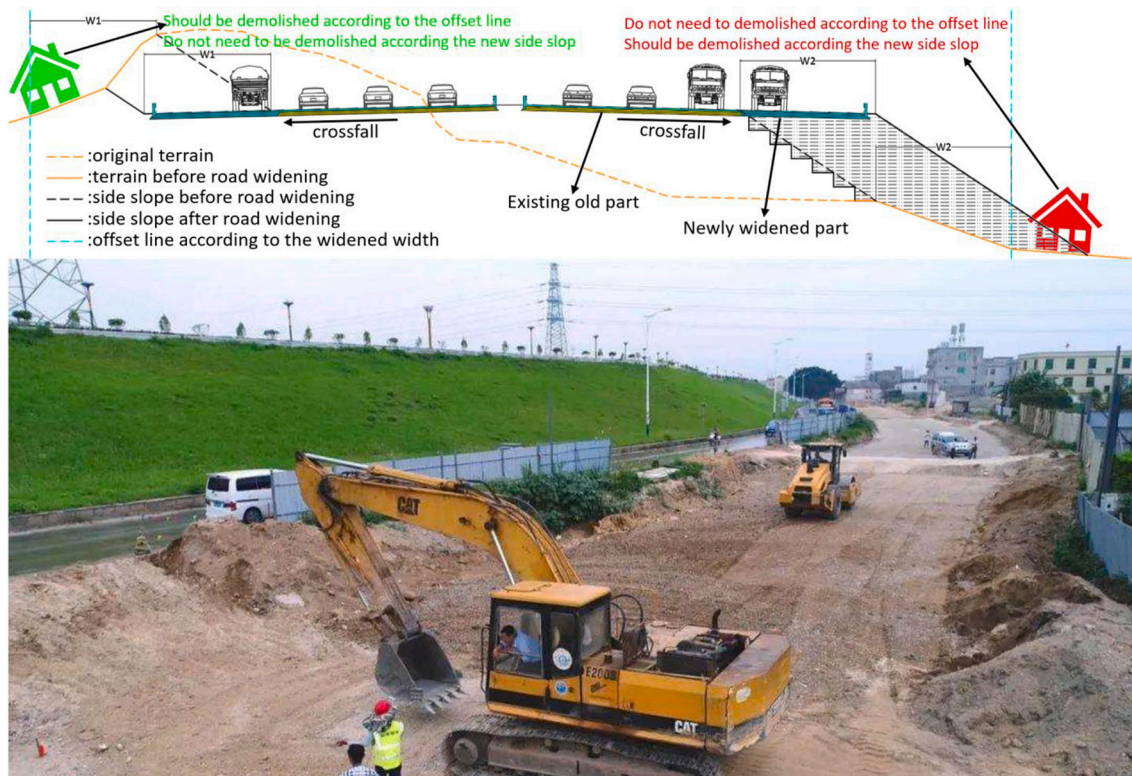


Fig. 1. Road widening and building demolition.

pollution, habitat change, and historical and socio-environmental factors. Using multi-criteria tools, the environmental impact assessment was quantified for alternatives of a road stretch using fourteen criteria to mitigate environmental impacts effectively. Sun, et al. [54] employed the road area as the proxy variable of road infrastructure construction and further divided the road reconstruction pattern into lengthening pattern and widening pattern, respectively, to evaluate the impact on urban air quality. The empirical result shows increasing road width has an emission-alleviating effect on air pollution. In addition, the research reveals that the effect of road lengthening on air quality is better than road widening in Eastern China. However, the improvement of road widening in Central and Western China is better than road lengthening. Finally, some studies focus on the influences of road widening on animals. Boyle, et al. [10] monitored the abundance and distribution of large mammals adjacent to a highway which was widening from a two-lane to a four-lane, divided highway over four years. They found that to meet the increasing traffic, road widening has fewer influences on large mammals to improve compared to new construction.

## 2.2. As-is BIM in the construction sector

As-is building information models (BIM) of existing buildings are valuable in the field of urban planning, historical structure information storage, project renovation, facility management, and building energy simulations [13]. Building an accurate and useful as-is model with geometric information and non-geometric information can leverage all kinds of data, such as point clouds, images, videos, 2D drawings, RFID data, to realise various applications in the field of architecture and infrastructure.

From the perspective of different raw data and creation methods for constructing as-is BIM, first, point clouds from laser scanners are always used. Wang, et al. [59] presented an automatic method to extract building geometries from unorganised point clouds to build as-is BIM models. Through data downsizing, boundary detection, and building component categorisation, building components can be recognised as individual objects and visualised as polygons. The proposed method can simplify and accelerate the as-is building model from the point cloud creation process. In addition to geometric information, semantic enrichment is also important for BIM models. Qiu, et al. [48] developed an adaptive down-sampling method for as-is BIM reconstruction considering semantic features using laser scanners, which can maintain scan points containing critical geometric or semantic information and only downsample scan points that do not contain critical information. Second, images are also very common raw data captured from cameras to build as-is BIM models. Lu, et al. [39] developed a semi-automatic image-driven system to recognise building objects and their materials based on a new neuro-fuzzy framework and an extensible texture library. The system can recognise buildings' beams, columns, windows, doors, and walls and their corresponding surface materials from a single image taken by a handheld digital camera and converted into as-is BIM in industry foundation classes (IFC) format. Chen, et al. [12] developed a semi-automatic image-based object recognition system for constructing as-is IFC BIM objects based on fuzzy-MAUT. The system can recognise buildings' indoor structure object types and their corresponding materials. Third, 2D drawing can be recognised to assist in creating the models. Lu, et al. [38] developed a semi-automatic and accurate digital twinning system based on images and CAD drawings for as-is BIM consisting of three modules: Building Framework Construction and Geometry Information Extraction Module, Building Information Complementary Module, and Information Integration and IFC Creation Module. Fourth, Radio Frequency Identification (RFID) also can assist other methods to create as-is BIM models. Valero, et al. [57] proposed an automatic method to construct 3D basic-semantic models of inhabited interiors such as walls, floor, ceiling, windows, doors, tables, chairs and cabinets using laser scanners with the help of RFID technologies. The proposed method performs selective and sequential segmentation from

point clouds through different algorithms that rely on the information provided by RFID tags. Finally, several applications are based on online map data. Jiang, et al. [27] proposed a systematic method to build as-is BIM models for highways in rural areas from online map data considering different road components. Abdelmaksoud, et al. [1] reconstructed the as-is BIM model of a historic building to analyse its slope stability and evaluate the defects of the superstructure. Through visualisation and numerical modelling, they proposed rehabilitation schemes for the historical building.

Several existing studies focus on optimising the work process of the as-is BIM. Wang, et al. [60] proposed a framework for scan-to-BIM to assist the BIM applications using the created as-is BIM. The framework includes four steps: identification of information requirements, determination of required scan data quality, scan data acquisition, and as-is BIM reconstruction. Chen, et al. [13] proposed a 2D proactive scan-planning framework for existing buildings based on laser scanners to create a scan plan before going to the construction site to improve the data collection process. The framework includes three modules: an information-gathering module, a preparation module, and a searching module, to build as-is BIM models. They compared a greedy best-first search algorithm, a greedy search algorithm with a backtracking process, and a simulated annealing algorithm based on actual building site drawings to find their strengths and weaknesses. Qiu, et al. [49] developed a scan planning method for existing buildings without BIM based on user-defined data quality requirements and genetic algorithms. A pre-scan is performed to quickly capture a preliminary point cloud of the building and segment the point cloud into planar segments. Then, a user-friendly graphical user interface is provided for users to define customised point cloud data quality requirements based on plane segments. Afterwards, a genetic algorithm is employed to find the optimal scan position and parameters that meet user-defined data quality requirements and achieve the minimal total scan time.

In addition to buildings, as-is BIM is also employed in other fields such as transportation infrastructure and MEP components. Cheng, et al. [14] presented a method to identify different types of components (rails, cross-sections, pipes, catenary equipment and refuges) and create parametric as-is BIMs for single-track railway tunnels using the Terrestrial Laser Scanning data automatically. The proposed method includes two core processes: point cloud classification and model parameters estimation. Lu and Brilakis [40] proposed a slicing-based object fitting method to generate the geometric digital twin of an existing reinforced concrete bridge from four types of labelled point clusters effectively and accurately. Adán, et al. [2] presented a 6D-based (XYZ + RGB) method to process dense coloured 3D points captured from terrestrial laser scanners to recognise the buildings' small MEP components on walls, such as sockets, switches, signs, extinguishers and others. After segmenting point clouds corresponding to building walls, a set of candidate objects are independently detected in colour and geometric spaces, and the original consensus procedure integrates these two results to infer recognition. After that, the identified objects are located and inserted into the as-is semantically enriched BIM model.

## 2.3. BIM and digital twin applications in the road engineering

A road is an alignment-based civil infrastructure rather than an entity-based structure [35]. Thus, the implementation of digitalisation technology such as digital and BIM in the road engineering sector has some differences compared with that in the building industry from the perspective of modelling methods, whole life cycle, and various applications. Generally, the road digitalisation should not only focus on a structure on one site, but also focus on the whole project along the road alignment and consider surroundings, environment, and GIS technology [19].

To create models for a road project, first, commercial BIM software can be employed. Biancardo, et al. [7] built parametric BIM models for road infrastructures using different visual programming software and

BIM tools and explored the interoperability of the software to extract and exchange information between these BIM tools. Second, some plugins based on commercial BIM can be developed to realise specific functions and make models for roads more efficiently. Vignali, et al. [58] employed I-BIM (Infrastructure Building Information Modelling) approach to upgrade a section of the road in the north of Italy, using Civil 3D software, Revit software, and a plugin they developed. The process included establishing a digital terrain model from point clouds, creating the horizontal alignment, creating the vertical alignment, building cross-sections, establishing the jacked tunnel, creating the roundabout, creating the 3D parametric model of the complete road, and viewing the infrastructure in the virtual space. Third, some systems are developed to edit, visualise and manage road models. Lee, et al. [35] developed a system to divide the 3D road BIM model according to the level required by users. Users could input the start and end points or set a constant interval unit on the road alignment to divide the road BIM model by segments. Each segment could be added with information such as earthwork volume (cut and fill), costs, and schedule. Fourth, for the existing roads, various algorithms are proposed to reconstruct models for the roads. Sometimes, the process can be regarded as a digital twinning process. Barazzetti, et al. [6] presented a two-step procedure to detect and classify roads automatically from LiDAR data to provide GIS layers with basic road geometry that were turned into parametric BIM objects. Justo, et al. [31] proposed a semi-automatic approach to extract and establish the BIM models for road elements from 3D point clouds, such as alignment, traffic signs, and guardrails in accordance with IFC 4.1 standard, along with the inclusion of some semantics via property sets. Soilán, et al. [52] proposed a semi-automated method to establish road alignment entities and the centreline of each road lane in IFC format from highway MLS-acquired LiDAR.

BIM can be implemented in the design phase of road engineering, but there are few digital twin-related applications. First, BIM can be employed to optimise road alignment. Bongiorno, et al. [8] proposed a 3D highway alignment optimisation approach based on the Particle Swarm Optimization method in a proper BIM environment, which could simplify the analysis of the different schemes, the final representation, and the eventual manual modifications. Kim, et al. [33] proposed an object-oriented 3D visualisation modelling method in accordance with ISO 10303 to assist highway alignment schemes comparison by cost estimating and duration scheduling automatically based on BIM. Zhao, et al. [64] proposed a highway alignment optimisation approach considering features of the project and its surroundings in a comprehensive 3D virtual environment based on BIM, GIS, semantic web technologies, and genetic algorithms. Second, BIM can assist in pavement designing by integrating design standards and structure analysis based on finite elements. Tang, et al. [55] proposed a platform integrating BIM-based highway three-dimensional visual modelling and design using Revit and pavement structural analysis based on finite elements in pavement engineering using ABAQUS. Tang, et al. [56] combined a 3D parametrically controllable road model established by Dynamo with the Mechanistic-Empirical Pavement Design Guide, which could provide the pavement structure analysis to reduce the mistake and repetition in pavement design. Third, some simulations can be conducted based on BIM, such as traffic simulation, to assist road component design. Castañeda, et al. [11] developed a BIM-based framework for traffic analysis and simulation for road intersection design, including BIM models and traffic information collection; BIM model configuration; BIM simulation, analysis, and calibration; BIM cost analysis and documentation; and alternatives comparison and recommendations. Jiang, et al. [28] proposed a DT (digital twin)-MCDM (multi-criteria decision making)-GIS (geographic information system) framework for sustainable urban road planning, considering building demolition and land use, traffic congestion, driving route selection habits, noise, and air pollutants comprehensively.

In the construction phase, BIM and digital twin also can be implemented to monitor and manage road projects. By leveraging drone

survey results, Lee, et al. [34] monitored the construction status of the earthwork and structure work through time-series images and overlapping of the 3D topographic information model with 2D computer-aided design (CAD) and 3D BIM design drawings. This process also can be regarded as a digital twinning process. Maksimych, et al. [41] developed a road construction complex automated control system integrating the processes of interaction control systems of road construction machinery based on road BIM. The system performed task control on the motion control and spatial position of construction machinery and its working mechanism and dispatched transportation operations in real-time.

In the operation and maintenance phase, BIM and digital twin can provide a digital, visual, integrated environment for the road project to conduct the whole process efficiently. Yu, et al. [62] proposed a method for organising, collecting, and fusing spatio-temporal data of the whole life cycle of roads based on the extended COBie standard to promote the link and interoperability of multi-source heterogeneous data; the new road operation and maintenance function requirements from the perspective of smart cities; a system called Road Intelligent Operation and Maintenance System which could support intelligent function requirements based on the system and a new generation of information technology. Bosurgi, et al. [9] proposed a method to present and elaborate road pavement condition information in an I-BIM environment. This process could simplify the representation and detailed description of survey information of pavement structural and functional conditions in a 3D environment by leveraging the potential of smart objects. Oretto, et al. [45] developed an efficient BIM tool to assist in road maintenance operations through the management of data generated from laboratory experiments for road pavement asphalt materials requiring the quality control of mixtures. An algorithm that interacted with 3D road models had been implemented to provide easy-to-read warning signals of road pavement structure in the road network for road management that might represent worst conditions due to poor mechanical and physical properties. By leveraging Lidar, unmanned aerial vehicles (UAV), traffic counting artificial intelligence, photogrammetric reconstruction technique based on a neural network, and sensors, Steyn and Broekman [53] developed a digital twin for a local road network considering advanced environmental data, physical data, and surface temperature data to assist in the maintenance of roads.

Additionally, BIM and digital twin can realise more complex and sustainable applications for road engineering and evaluate the road comprehensively. Shi and Lv [51] proposed a framework to evaluate green highways based on Big Data GIS and BIM technology, considering design, construction, and maintenance. By using BIM technology and IFC format data, Aranda, et al. [4] considered sunny and shady areas as a parameter in the iterative road design of modifying the road's geometric elements to test various schemes until the road's surface area in the shady area is minimised to improve the road safety. Marzouk, et al. [42] proposed a BIM-based approach to assess the environmental impacts on road construction projects considering the whole life cycle, including the manufacturing phase, transportation phase, construction phase, maintenance phase, operational phase, recycling phase, and deconstruction phase.

#### 2.4. The gaps in the literature review

From the literature review, some gaps can be discovered:

- 1) Most studies focus on as-is BIM applications of buildings or infrastructure. No study can comprehensively utilise as-is BIM of roads and buildings synthetically in the field of road engineering to assist in road widening and estimating its influences on surroundings.
- 2) Few studies propose feasible algorithms and methods to build as-is BIM models for roads, and new BIM models for widened road considering road components (road alignment, central reserve, hard strip, lane, hard shoulder, verge, side slope, crossfall, and

superelevation) in accordance with road engineering expressions based on online map data rather than field surveys in the preliminary design phase.

- 3) No study proposed a feasible approach to estimate building demolition quantity and costs caused by road widening using as-is BIM based on online map data, policy, and government statistics.

Thus, the following sections will fill the gaps.

### 3. Methodology

Road widening projects should be conducted based on the existing old road to construct new pavements, subgrades, and side slopes. In the process of road widening, building demolition may occur, which can incur some costs. There are two traditional methods to estimate building demolition costs. One is by offsetting the boundary of the old road outwards by a specific value on the 2D map, and the other one is by field surveys. However, the former does not consider the alignments, cross-sections and their components, crossfall, superelevation, and side slopes of the 3D road, which can generate inaccurate boundaries for the new road and wrong building demolition, as shown in Fig. 2. The latter is too labour-intensive, costly, and time-consuming in the preliminary design phase. Thus, this paper proposes a systematic method as a compromise to build an as-is BIM model for the existing buildings and the old roads from online map data, policy, and government statistics and establish the BIM model for the newly widened road based on the old road's as-is BIM model. Then, the demolition are estimated by clash detections between the buildings' as-is BIM models and the road BIM model.

#### 3.1. Road fitting algorithm and as-is BIM model for road widening

A workflow is proposed to build the as-is BIM model for the target road, as shown in Fig. 3. After downloading the aerial photographs with the coordinate file (e.g. tif + tfw, jpg + jgw format), road marking pixels can be detected and obtained according to their (R, G, B) values, where R denotes red, G denotes green, and B denotes blue. Several pixels of the road marking can be selected dispersedly in advance to find the characters of their (R, G, B) values. For example, the road markings are

greyish-whites. Thus the absolute values of differences between the R and G, G and B, and B and G of each road marking pixel are very small (e.g.  $abs(R-B) \leq 15$  &  $abs(B-G) \leq 15$  &  $abs(G-R) \leq 15$ ) and its R,G,B values are within a certain range where the colour is not too dark or white (e.g.  $140 \leq R,G,B \leq 200$ ). Pixels that meet the conditions will be filtered out and converted to white (RGB = (255,255,255)), while other pixels will be converted to black (RGB = (0,0,0)). Thus, an image called Road marking image 1 can be produced by the black or white pixels, as shown in ② in Fig. 4. After that, the white pixels outside road pavement and the white pixels that do not represent the road markings can be recognised easily compared to the aerial photographs and are coloured in black manually to build the Road marking image 2, as shown in ③ in Fig. 4.

Afterwards, the white pixels of the Road marking image 2 are converted into point clouds according to its coordinate file, as shown in Fig. 5. The image pixels are counted from the upper left corner as the starting pixel, and sometimes the starting pixel is not a full pixel. The green point is the start corner of the image; the orange point is the upper left corner of the full starting pixel; the blue pixels are the centre points of each full pixel. If a pixel is white, it is a pixel of the road markings, and its centre point will be extracted to represent the pixel. Then, all the centre points are assigned to the right coordinates according to the coordinate file (e.g. jgw or tfw). The coordinate file can provide the relationship between the green point and its geographical coordinates (the black point). Thus, the geographical coordinates of all the centre points of the pixels on the Road marking image 2 can be determined by Eqs. (5) and Eqs. (6), where  $i_0, j_0, i, j, d, n, m, x_0, y_0$ , can be shown in Fig. 5. In the Eqs. (5) and (6),  $d$  denotes how many meters does the side length of a pixel (square) represents in the real world, and  $x_0, y_0$  denotes the coordinates of the upper-left corner of the image in the real world. The aerial photograph is downloaded from a map database with its coordinate file. For example, the aerial photograph can be downloaded in jpg + jgw or tif + tfw formats.  $d, x_0, y_0$  can be obtained from its coordinate file like jgw, tfw.  $i_0$  and  $j_0$  denotes, the position of the image's upper-left corner in its corresponding full pixel, since the image may not start from a full pixel.  $i_0$  and  $j_0$  are represented by the ratio compared to a full pixel according to the position rather than a specific coordinate. For example,  $i_0$  is 0.6 pixel and  $j_0$  is 0.7 pixel. Thus,  $0 \leq i_0$  and  $j_0 \leq 1$ .  $n$  and  $m$  are determined by how many pixels the image has. Thus, all the centre points (blue points) can be moved to their corresponding geographical

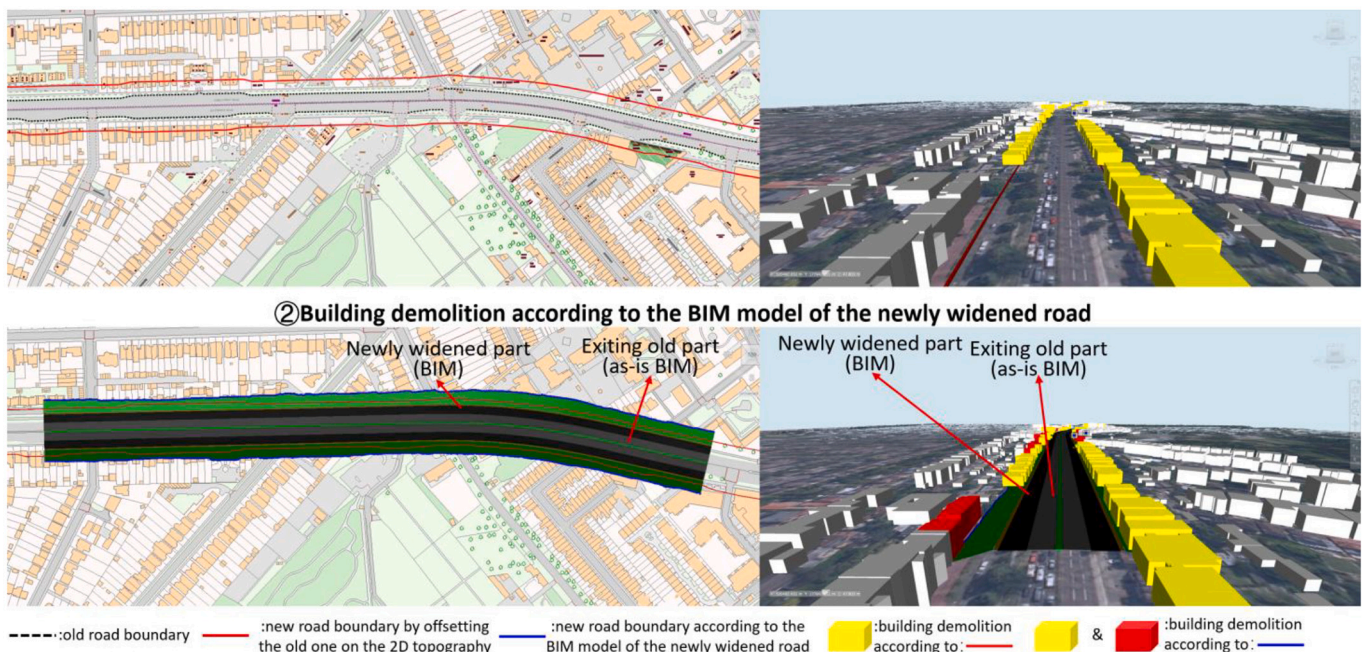


Fig. 2. Building demolition estimation by 2D map (①) and by BIM (②).

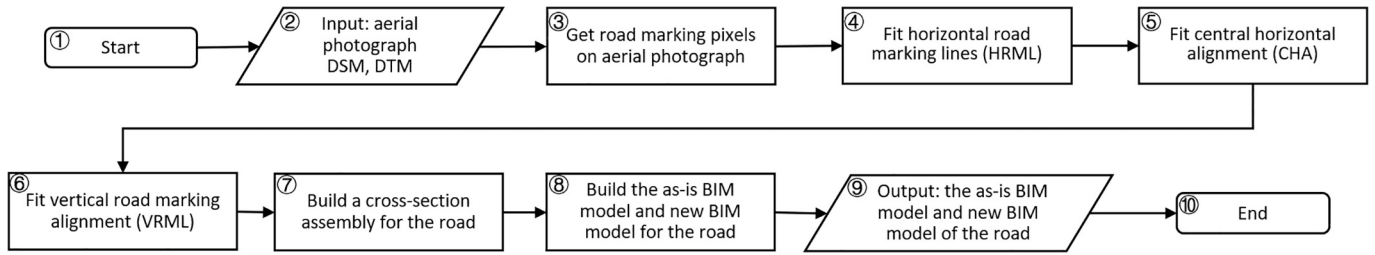


Fig. 3. Workflow for building the road's as-is BIM model and new BIM model.

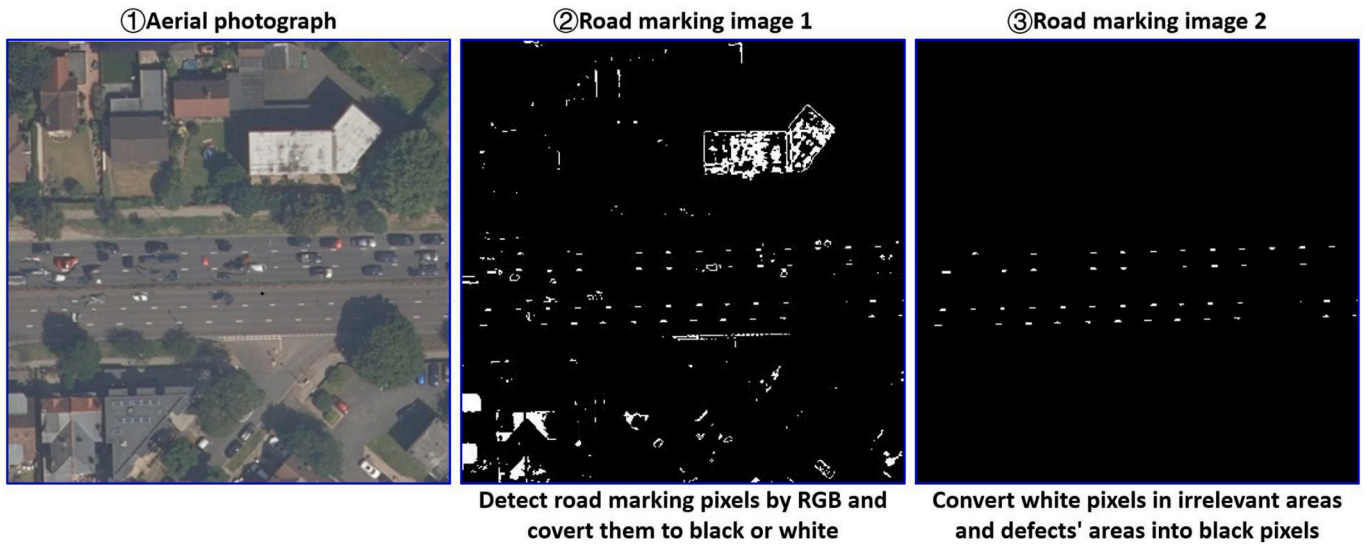


Fig. 4. Road marking pixels extraction process using aerial photographs.

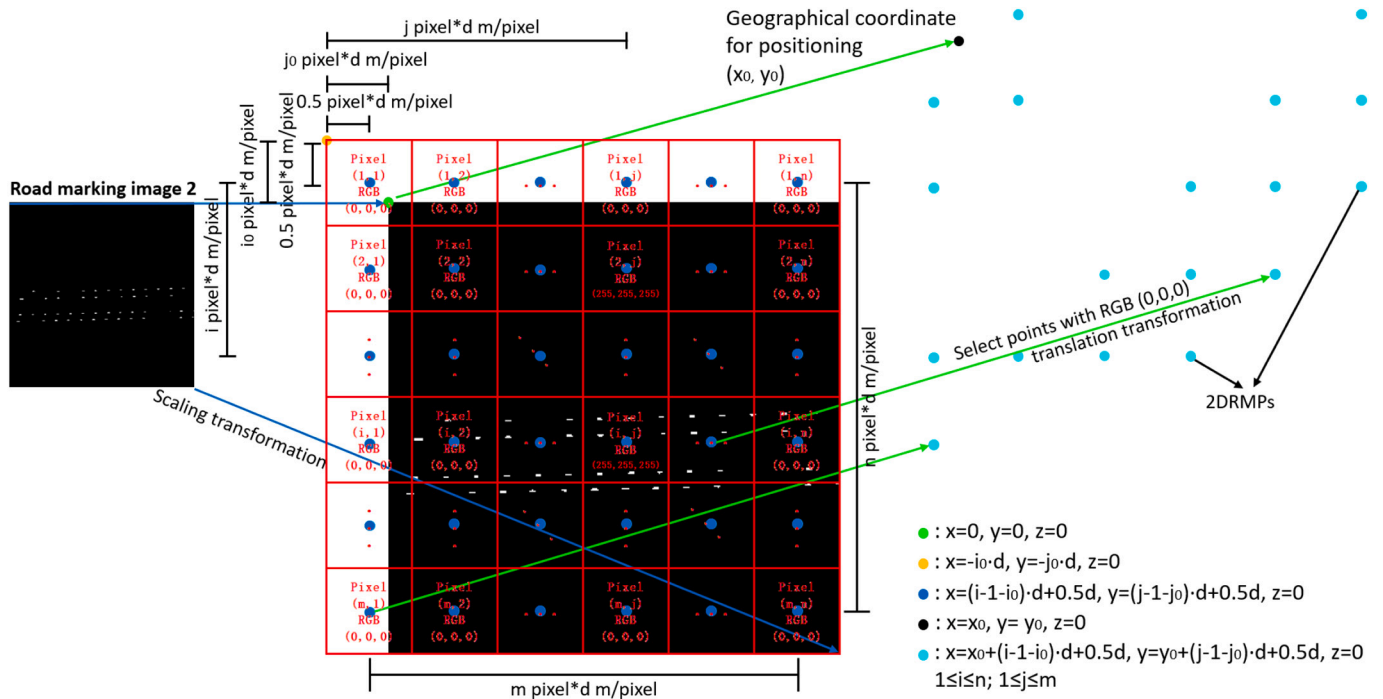


Fig. 5. 2D road marking points (2DRMPs) with the right geographical coordinates from road marking pixels.

coordinates to become 2D road marking points (2DRMPs) which are cyan points in Fig. 5. The z coordinates of all 2DRMPs are zero. Thus, all the centre points (blue points) can be moved to their corresponding geographical coordinates to become 2D road marking points (2DRMPs) which are cyan points in Fig. 5. The z coordinates of all 2DRMPs are zero.

$$x = x_0 + (i - i_0 - 0.5) \cdot d \quad 1 \leq i \leq n \quad (5)$$

$$y = y_0 + (j - j_0 - 0.5) \cdot d \quad 1 \leq j \leq m \quad (6)$$

After obtaining 2DRMPs from digital image processing, 2DRMPs can get elevations from DSM to get 3D road marking points (3DRMPs). Since there are many vehicles on the road, the original DSM can be very bumpy. Since most 3DRMPs are on the pavement rather than on the vehicles, they are employed to make a flat DEM (digital elevation model) called road marking DEM (RMDEM), as shown in Fig. 6. 2DRMPs are employed to fit horizontal alignments, and then the elevations along the alignment are extracted from RMDEM. However, the outermost fitted horizontal alignments for road marking are near the boundary of the RMDEM, and in some areas, it can go out of the boundary of the RMDEM where there are no elevation data, as shown in ① in Fig. 7. Thus, RMDEM is mosaicked on the DSM to establish mosaic DSM (MDSM), where the values are the same as the RMDEM within the range of RMDEM, and the values are the same as DSM beyond the range of RMDEM, as shown in ② and ③ in Fig. 7.

Then, smoothing splines are employed to fit the horizontal road marking lines using 2DRMPs, and a smoothing spline can be expressed by Eqs. (7) (④ in Fig. 8), where  $f$  is any twice-differentiable function on  $[a, b]$  which is the function of the smoothing spline, and  $\lambda$  is the smoothing parameter. The smoothing spline endeavours to minimise  $S(f)$ . The parameter  $\lambda$  is defined between 0 and 1.  $\lambda = 0$  produces a least-squares straight-line fit to the data, and  $\lambda = 1$  produces a cubic spline interpolant that goes through all the data points. The quality of the fitting result can be evaluated by Eqs. (8) to Eqs. (11), where  $RMSE$  is the root mean squared error,  $R - square$  is coefficient of determination,  $SSR$  is the sum of squares of the regression,  $SST$  is the total sum of squares,  $y_i$

is the original value,  $\bar{y}_i$  is the average value of the original values, and  $\hat{y}_i$  is the fitted value. The range of the “coefficient of determination”  $R - square$  is  $[0, 1]$ . The closer to 1 it is, the stronger the interpretation ability of the variables of the equation is for  $y$ , and the model fits the data better. The smooth spline will follow the overall trend of the 2DRMPs; thus, the local loss of the points has no obvious influence on the overall shape of the smoothing spline. Hence, it is acceptable to delete appropriate numbers of points when convert Road marking image 1 into Road marking image 2 to remove the defects (e.g. vehicle points). After fitting the road marking lines using the 2DRMPs and smoothing splines, the points on each smoothing spline per meter along the x-axis are extracted (② in Fig. 8). Using the extracted points, the horizontal road marking alignment (HRMLs) are established (③ in Fig. 8). In addition to HRMLs, the central horizontal alignment should be fitted. If the central horizontal alignment (CHA) is fitted by a smoothing spline using the 2DRMPs of the nearest road markings on the left and right sides of the central alignment, it will fluctuate due to the missing points on the one side and existing points on the other side (① in Fig. 9). Thus, the points on the nearest smoothing splines on the left side and right side per meter along the x-axis are employed to fit the CHA (④ in Fig. 8 and ② in Fig. 9). After the fitting process, a smoothing spline for CHA can be obtained. Then, the points on the smoothing spline per meter along the x-axis are extracted (⑤ in Fig. 8), and the CHA can be established by the extracted points (⑥ in Fig. 8).

$$S(f) = \lambda \sum_{i=1}^n (y_i - f(x_i))^2 + (1 - \lambda) \int_a^b (f''(x))^2 dx \quad (7)$$

$$RMSE = \sqrt{\frac{1}{m} \sum_{i=1}^m (y_i - \hat{y}_i)^2} \quad (8)$$

$$SSR = \sum_{i=1}^m (\hat{y}_i - \bar{y}_i)^2 \quad (9)$$

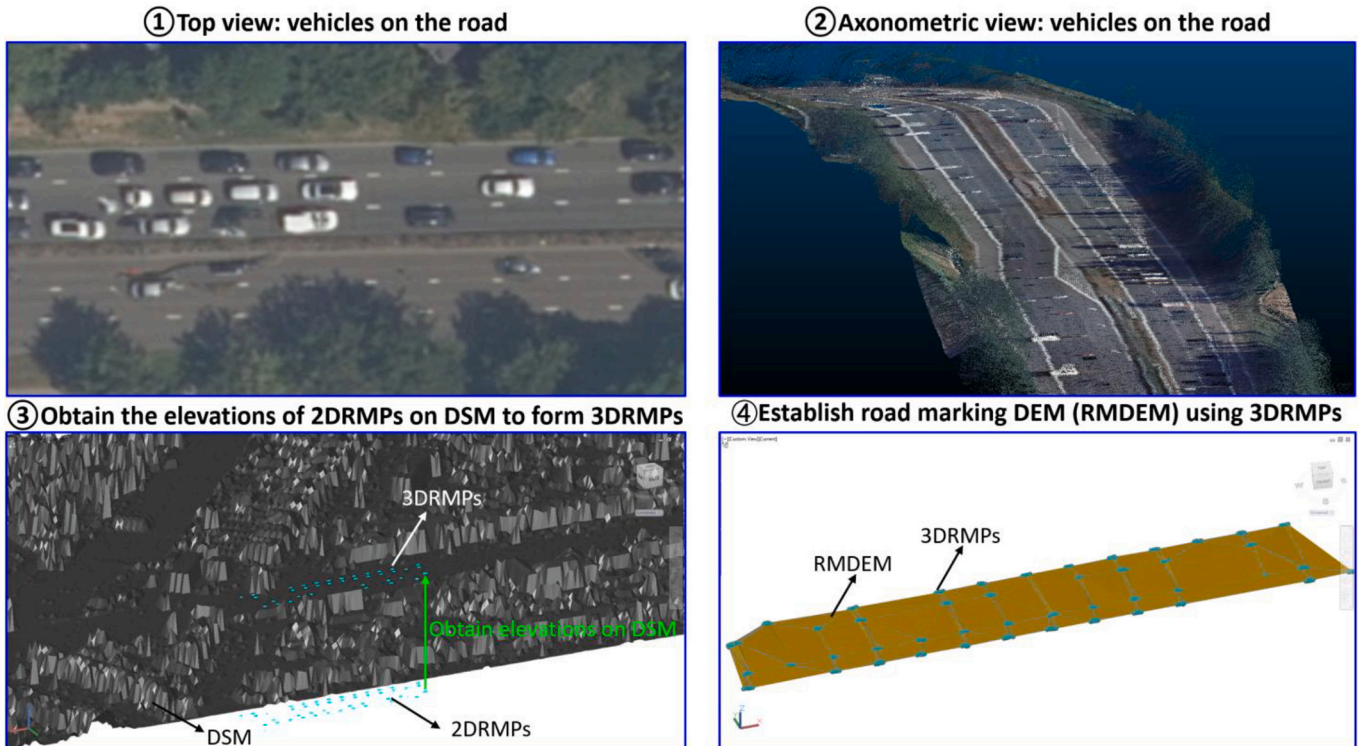


Fig. 6. 2DRMPs' elevations extraction and RMDEM establishment.

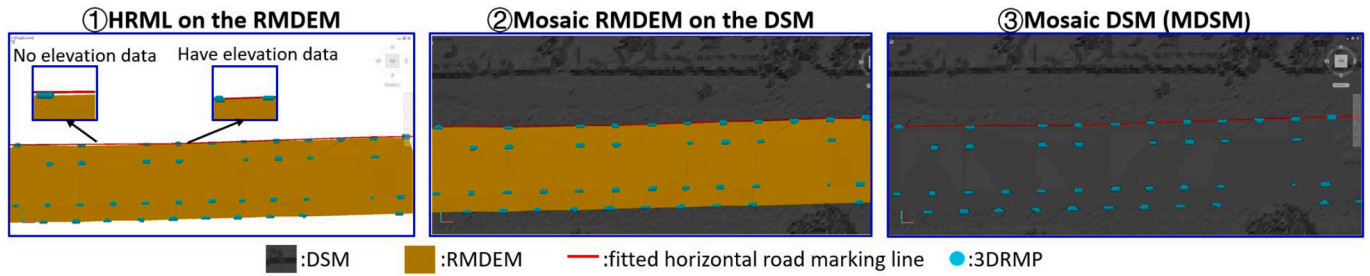


Fig. 7. MDSM creation process.

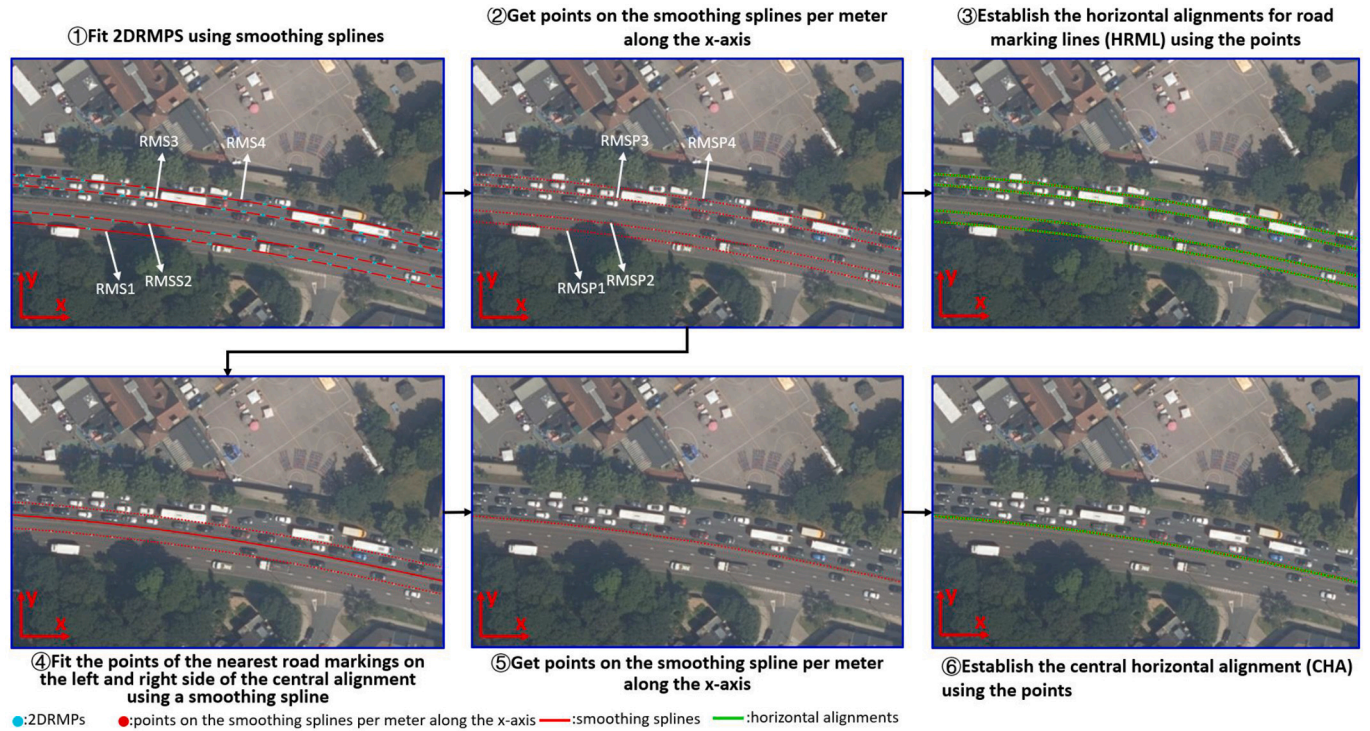


Fig. 8. Horizontal alignments fitting process for road markings and central alignments using 2DRMPs.

$$SST = \sum_{i=1}^m (y_i - \bar{y}_i)^2 \quad (10)$$

$$R - square = \frac{SSR}{SST} \quad (11)$$

The next step is to establish the vertical alignments for the HRMLs. The elevations ( $E_1$ ) on the MDSM along the HRMLs are extracted, and the points ( $E_1, S$ ) can be obtained where  $S$  denotes the stations of HRMLs (① in Fig. 10). After that,  $E_1$  is filtered by Hampel filter to remove the outliers and defects on the pavements (② in Fig. 10). The Hampel filter process can be shown by Eqs. (12)-Eqs. (15), where  $x_i$  denotes the original data ( $E_1$ ),  $y_i$  denotes filtered results,  $n$  and  $t$  should be given appropriate values. The points ( $E_1, S$ ) after the Hampel filter can be expressed by ( $E_2, S$ ). After that, smoothing splines are employed to fit the points ( $E_2, S$ ) (③ in Fig. 10). Then the points along each smoothing spline ( $E_3-S$ ) per meter are extracted, and the points can be expressed by ( $E_4, S$ ) (④ in Fig. 10). Afterwards, the vertical road marking alignment (VRML) of each HRML can be established by ( $E_4, S$ ) and can be expressed by  $E_4-S$  (⑤ in Fig. 10).

$$W_i^n = \{x_{i-n}, \dots, x_i, \dots, x_{i+n}\} \quad (12)$$

$$m_i = median \{x_{i-n}, \dots, x_i, \dots, x_{i+n}\} \quad (13)$$

$$y_i = \begin{cases} x_i & |x_i - m_i| \leq tS_i \\ m_i & |x_i - m_i| > tS_i \end{cases} \quad (14)$$

$$S_i = 1.4826 \times median_{j \in [-n, n]} \{|x_{i-j} - m_i|\} \quad (15)$$

After HRMLs and VRMLs are determined, the cross-section assembly is established, as shown in Fig. 11. VL denotes vertical control lines, and HL denotes horizontal control lines. The position of VL7 is determined by CHA. The positions of VL4, VL5, VL9, and VL10 are determined by HRMLs. Moreover, the positions of HL1, HL2, HL3, and HL4 are determined by VRMLs. P5, P6, P9, P10 are the intersections between VL4 and HL1, VL5 and HL2, VL9 and HL3, VL10 and HL4, respectively. L5 and L9 are the lines linking P5 and P6, P9 and P10, respectively. Thus, the L5, L9, and their corresponding pavements (old lanes) of the existing old road can be controlled flexibly by HRMLs and VRMLs, and the crossfalls and superelevations can be determined automatically. Other VLs are determined by the red VLs (VL4, VL5, VL9, and VL10) and the corresponding D values (D1 to D4). D values can be determined by aerial photographs and highway design standards. P2, P3, P4, P7, P8, P11, P12, P13 are the intersections between extended lines of L5 or L9, and corresponding VLs and links between these points can be established (L2, L3, L4, L6, L7, L8, L10, L11, L12). L1 and L13 are the links with an appropriate slope value from P2 and P13, respectively. The P1 and P14



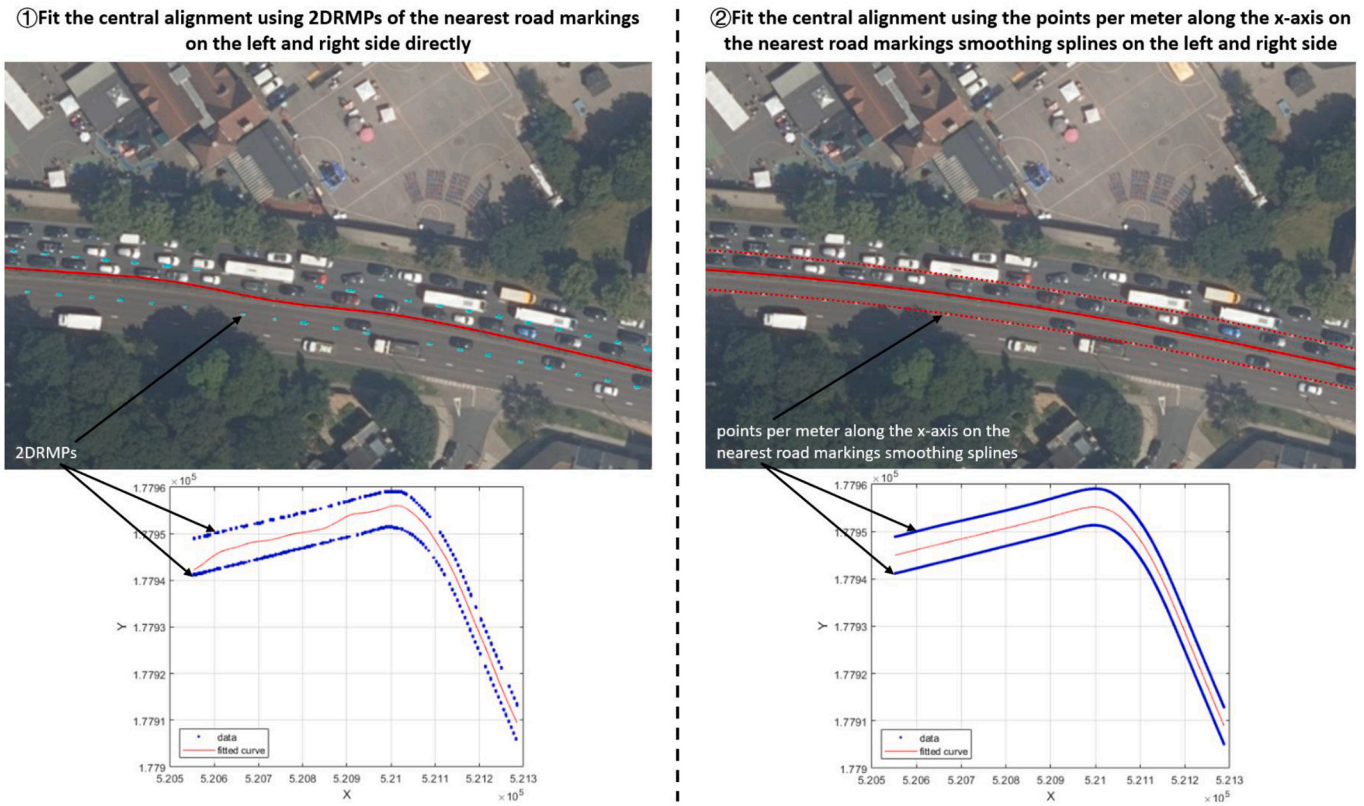


Fig. 9. Reason for the central alignment fitting using the points per meter along x-axis on the two adjacent alignments rather than 2DRMPs.

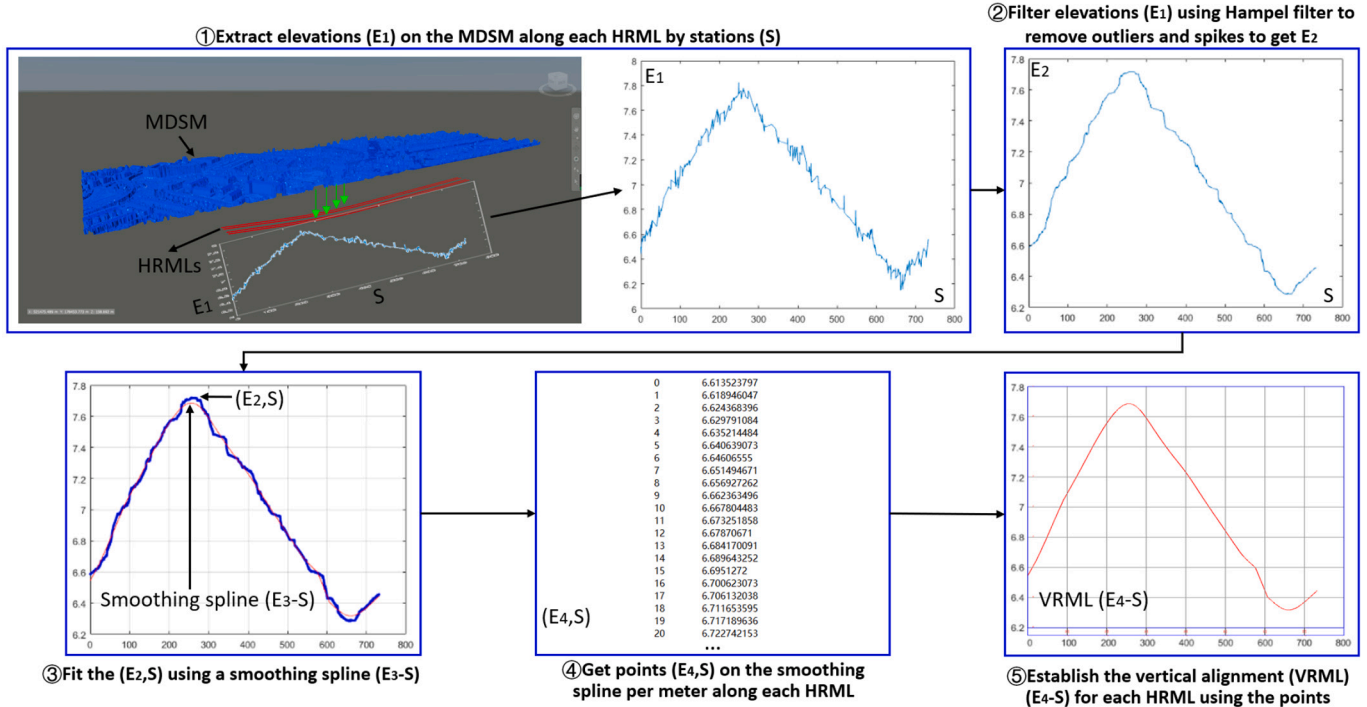


Fig. 10. Method for vertical alignment (VRML) creation of each HRML.

are the intersections between the terrain line and L1, and the terrain line and L13, respectively. Based on the links, various road components such as central reserves, pavements (including hard strips, lanes, and hard shoulders), verges, and side slopes can be established. The road's as-is

BIM model and new BIM model can be established by sweeping the cross-section assembly along HRMLs and VRMLs, where HRMLs control the x-y position and VRMLs control the elevation. In addition, the thickness of the pavement can be set to an appropriate value. Useful

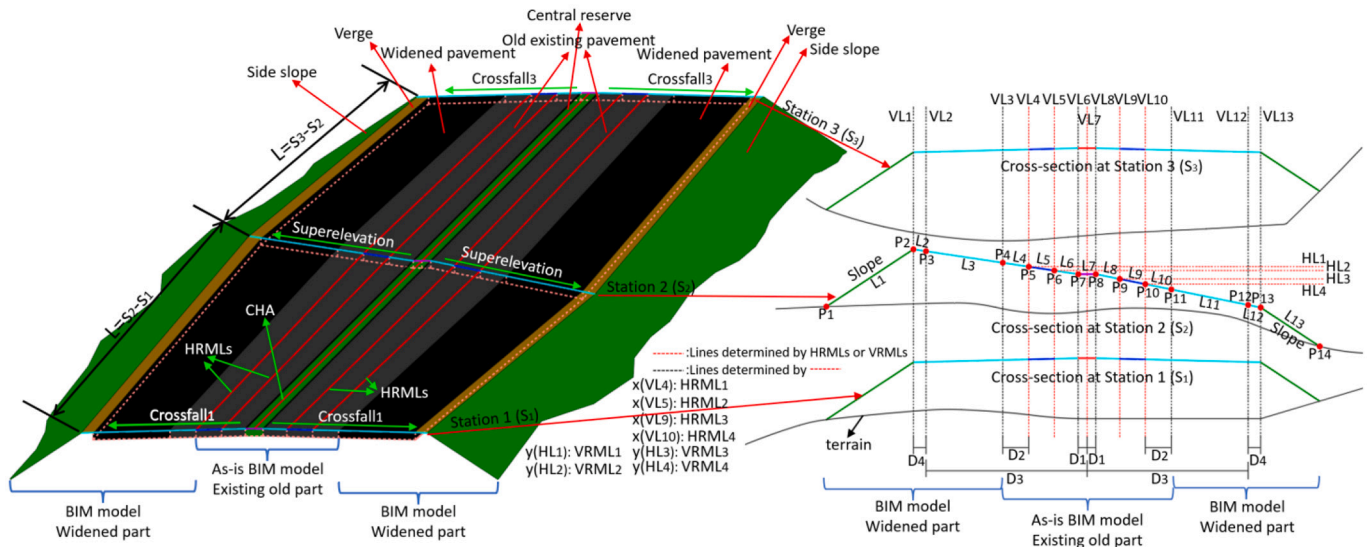


Fig. 11. Creation process of road's as-is BIM and new BIM model.

information can be added to the road as-is BIM and BIM model. Between the VL3 and VL11, the model is the as-is BIM model for the existing old road, and the other parts of the model are the road BIM models for the newly widened parts established according to the roads' as-is BIM model. The LoD (level of detail) of the road BIM model can reach LoD 200 in this research, considering various basic road components mentioned above. The components are detachable from the road BIM model with corresponding attributes, including BaselineName, CorridorName, HorizontalBaseline, RegoinName, VerticalBaseline, AssemblyStartStation, AssemblyEndStation, ModelType, Road-Componet (central reserve, pavement, verge, side slope), RoadPart (existing old part, widened part), Side (Left, Right, Middle), and Volume.

Using the proposed method, the road BIM model even can reach LoD 300, considering detailed drainage systems (such as ditches and culverts), traffic safety facilities, road markings, etc., which are not very important for building demolition estimation and are not discussed in this research [16,20,24].

### 3.2. Buildings' as-is BIM model

Road widening can cause demolitions of some existing buildings. In order to estimate the building demolition, establishing buildings' as-is BIM model is the first step. The overall workflow can be shown in Fig. 12. Topographic ordnance survey data and map data can be

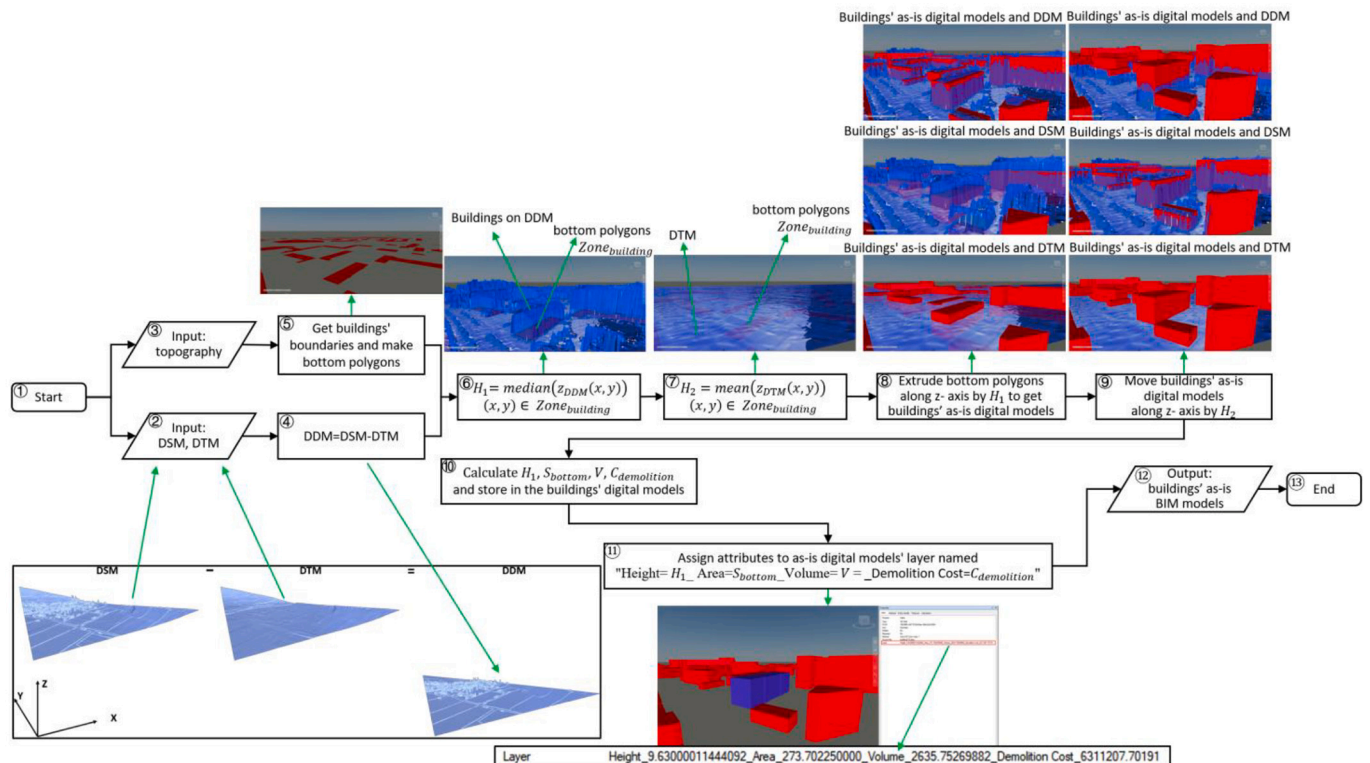


Fig. 12. Workflow for buildings' as-is BIM models creation.

obtained from different sources such as Digimap [18,36], Google Map, Google Earth, OpenStreetMap, ArcGIS, etc. In this research, 2D boundaries of buildings in the topography, Digital Terrain Model (DTM), and Digital Surface Model (DSM) data can be obtained from Digimap (②, ③ in Fig. 12). Points on DTM and DSM can be described by coordinates (x, y, z), where x denotes the coordinate of the point on the West-East horizontal axis, y denotes the coordinate on the South-North horizontal axis, and z denotes the height of the point compare with the horizontal plane. The differences between the z values of every two points with the same x and y coordinates on the DSM and DTM, respectively, can be calculated. The x, y, and the differences between the z values can produce a new kind of DTM, which is called the digital difference model (DDM), as shown in Eqs. (1) (④ in Fig. 12). DDM can be expressed by raster data in GIS. The boundaries of buildings in the topography can form 2D polygons, which represent the bottom of the building (⑤ in Fig. 12). Inside the boundary of each building ( $Zone_{building}$ ), the z value of each cell on the DDM raster can be calculated, and the median of the z values ( $H_1$ ) is used to describe the height of the building, as shown in Eqs. (2) (⑥ in Fig. 12). In addition, inside the boundary of each building ( $Zone_{building}$ ), the z value of each cell on the DTM raster can be calculated, and the mean of the z values ( $H_2$ ) can be calculated by Eqs. (3) to represent the elevation of each building's bottom (⑦ in Fig. 12). Then, the simple as-is digital model of buildings can be expressed by the 3D boxes by extruding the 2D polygon of the building's bottom (bottom polygon) along the z-axis according to the building heights (median of the z values in the  $Zone_{building}$  on the DDM) (⑧ in Fig. 12). The reason for using the median of the z values rather than the average z values in the  $Zone_{building}$  on the DDM to represent the height of a building is shown in Fig. 13. The circumstance in ① in Fig. 13 is the ideal circumstance in which the 2D building boundary can exactly fit the building's bottom in DDM, and the building has a flat roof. The z values in the  $Zone_{building}$  on the DDM are the same as their median and average values and can be used to describe the building height. In ② in Fig. 13, the building has a pitched roof. In ③ in Fig. 13, the top of the building is much smaller than

the bottom of the building. Both the median and the average value of the z values in the  $Zone_{building}$  on the DDM can approximately describe the height of the building to make an as-is digital model in ② and ③ in Fig. 13. However, in ③ in Fig. 13, there are slight deviations between the 2D building boundary and the building on the DDM. Thus, the red surface (top of DDM within the 2D building boundary ( $Zone_{building}$ )) can get the z value of the ground on the DDM. Similarly, due to the deviation, in ④ in Fig. 13, the red surface can get the z value of connected buildings, which is very tall or very low. Thus, in ③ and ④ in Fig. 13, the red surface can have very large or small z values, which can affect the average z values in the  $Zone_{building}$  on the DDM a lot. But the median value cannot be significantly affected by the very large or small z values due to the deviations. Therefore, the median of the z values in the  $Zone_{building}$  on the DDM is appropriate to describe the height of the building, and it is not appropriate to use average z values in the  $Zone_{building}$  on the DDM. Afterwards, the simple buildings' as-is digital models can be produced in batches automatically by extruding the bottom polygons according to the median of the z values. After that, the building's as-is digital models are established with appropriate heights, but the elevations of their bottoms are all zero. After that, the buildings' as-is digital models are moved along the z-axis by  $H_2$  (⑨ in Fig. 12). In this way, the buildings' as-is digital models are moved to DTM with appropriate elevation.

After establishing as-is digital models of existing buildings, information of the buildings, such as the height, area of the bottom, and volume, can be calculated and stored in the buildings' as-is digital models to generate independent buildings' as-is BIM models. The demolition costs ( $C_{demolition}$ ) of a building also can be calculated and stored in the buildings' as-is BIM models (⑩ in Fig. 12). The number of storeys of each building can be obtained by dividing the height of each building by the average floor-to-floor height of a building. To estimate the demolition costs, the government statistics of the building price should be found. Then, the demolition costs ( $C_{demolition}$ ) of a building can be calculated by Eqs. (4), where  $\mu$  denotes the amplification factor from the

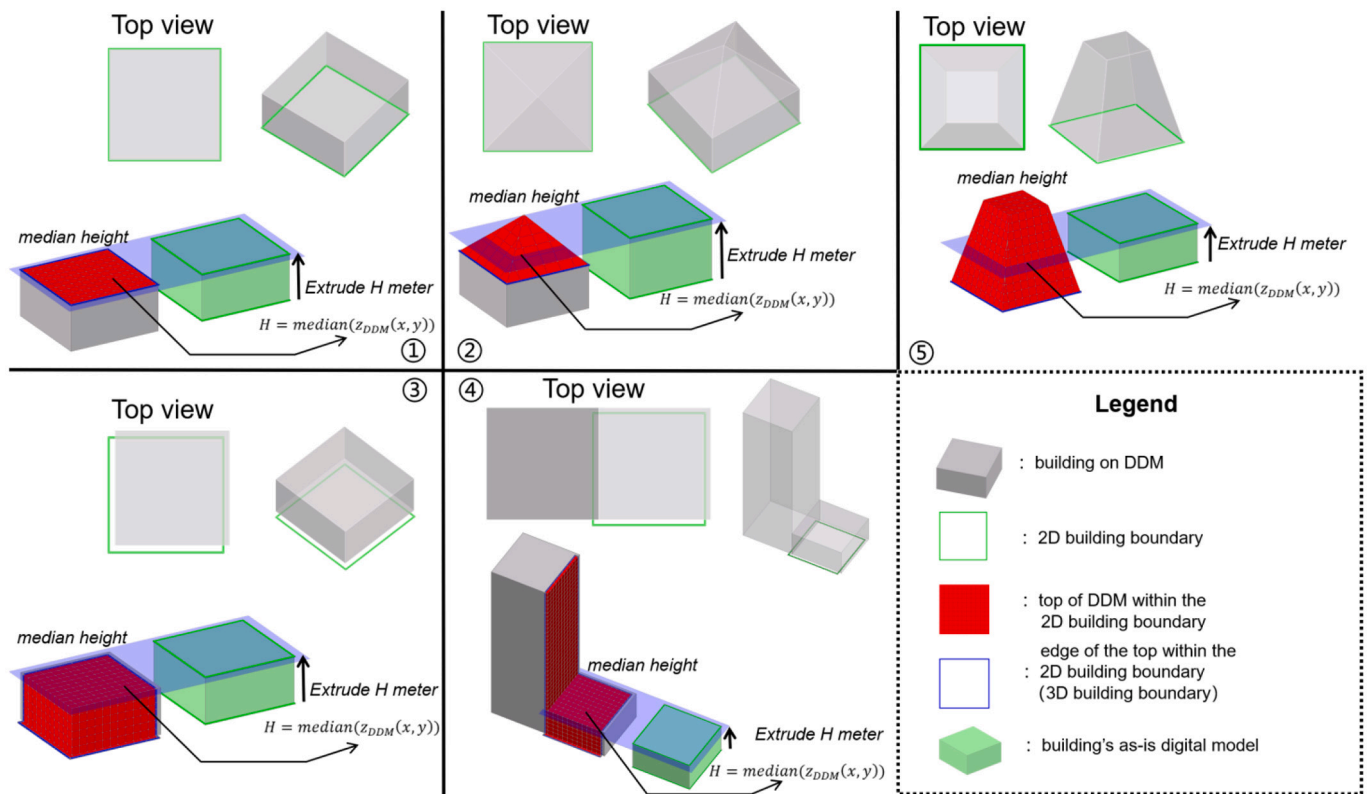


Fig. 13. Reason for assigning the median value of DDM to building height.

building price to the building demolition costs,  $V$  denotes the volume of the building's as-is BIM models,  $h$  denotes the floor-to-floor height of a building,  $S_{bottom}$  denotes the area of the bottom of the building, and  $p_{uld}$  denotes the up-to-date average price per square meter of properties in the target area.  $\mu$  is employed to consider the compensation and relocation of residents affected by the demolition. Sometimes the up-to-date average price per square meter of buildings in the target area is not available. Historical data can be used to predict  $p_{uld}$ . Generally, for road construction, if the road occupies a building partially, the building is totally demolished. For the convenience of clash detections in Section 3.3, different attributes can be assigned to as-is BIM models' layers, and the layers can be named as "Height= $H$ \_ Area= $S_{bottom}$ \_Volume= $V$ \_Demolition Cost= $C_{demolition}$ ", where  $H$ ,  $S_{bottom}$ ,  $V$ , and  $C_{demolition}$  can be expressed by Eqs. (4) in Fig. 12). The buildings' as-is BIM models can reach LoD 100, since the models are extruded boxes representing the envelopes of the buildings without considering various types of roofs or openings (such as windows and doors) [16,20,24]. Each building BIM model is independent, but there are no more detailed detachable components in each BIM model. All the attributes are stored in each BIM model, including volume, height, area, demolition cost, etc.

$$z_{DDM}(x, y) = z_{DSM}(x, y) - z_{DTM}(x, y) \quad (1)$$

$$H_1 = \text{median}(z_{DDM}(x, y)) \quad (x, y) \in \text{Zone}_{building} \quad (2)$$

$$H_2 = \text{mean}(z_{DTM}(x, y)) \quad (x, y) \in \text{Zone}_{building} \quad (3)$$

$$C_{demolition} = \mu \frac{V}{h} \bullet p_{uld} \bullet S_{bottom} = \mu \frac{V \bullet p_{uld}}{h} = \mu \frac{H_1}{h} \bullet p_{uld} \bullet S_{bottom} \quad (4)$$

### 3.3. Building demolition and costs estimation

After that, the buildings' as-is BIM models, road's as-is BIM model, and new BIM models of the widened road are imported into Navisworks to support a clash detection process (2 and 3 in Fig. 14). The clash detection is conducted between two groups of entities. The buildings' as-is BIM models are the first group, and the road's as-is BIM model and road new BIM models are the second group. Then, the clash detection report can be exported (4 in Fig. 14). Since some information of the buildings and road is stored in the models, the information of two entities clashing with each other can be obtained to evaluate the situation of the building demolition. In the clash detection report, only some properties will be displayed, such as layers. Since the layers of all building's as-is BIM models are named as "Height= $H$ \_ Area= $S_{bottom}$ \_Volume= $V$ \_Demolition Cost= $C_{demolition}$ ", the layer properties and their values can be extracted from the clash detection report, and the height, bottom area, volume, and demolition cost of each building clashing with the widened road can be obtained (5 in Fig. 14). Therefore, the total amount of demolition quantity and the total building demolition costs can be calculated. (6 in Fig. 14). In addition, since the road BIM models are detachable considering road components, which component has a clash detection with a building can be obtained from the clash detection reports. In the position where the clash detection

occurs between the road's side slop and a building rather than other road components (verge, hard shoulder, lane) and a building, retaining walls can be considered to be built to replace the side slopes to reduce building demolition.

## 4. Case study

The target research area is located in the place called Hounslow, which is a large suburban town in West London. The coordinates based on OSGB 1936 / British National Grid (EPSG:27700) of the lower-left and upper-right areas of the study area are shown in Fig. 15. The target road is called M4, which is a two-way six-lane motorway, and it can be widened to a two-way eight-lane motorway. There are low-rise residential and public buildings along both sides of the road in the target research area. The original map data, including DSM, DTM, topography, and aerial photographs, were downloaded from Digimap [18,36], as shown in Fig. 16. The proposed method is mainly implemented in MATLAB R2020B by programming. QGIS 3.18.2 is employed to process original DSM and DTM data, Civil 3D 2021 is employed to build BIM models, and Navisworks Manage 2021 is employed to conduct clash detection.

According to the government data, only the average price of properties per square meter in Hounslow in 2016 can be obtained, which was 5969 £/m<sup>2</sup> [21]. In addition, the average price of a property in each month of 2016 and in July 2021 can be obtained, as shown in Fig. 17 [43]. The up-to-date average price per square meter of properties in the target area ( $p_{uld}$ ) can be expressed by Eqs. (16), where  $p_{July\ 2021}$  denotes the average price per square meter of properties in July 2021,  $p_{2016}$  denotes the average price per square meter of properties in 2016 (5969 £/m<sup>2</sup>),  $P_{July\ 2021}$  denotes the average price of a property in July 2021, and  $P_{i, 2016}$  denotes the average price of a property in each month in 2016. The result of  $p_{July\ 2021}$  is 6385.23 £/m<sup>2</sup>, as shown in Table 1. In London, space standards for dwellings require buildings to have 2.5 m floor-to-ceiling height. An assumption of 0.7 m between ceiling and floors has been made. Thus, for each storey, the floor-to-floor height is usually 3.2 m ( $h$  in Eqs. (4)) [44]. Then the number of storeys of a building can be calculated by dividing the height of the building by 3.2 m. According to the UK policy, an owner-occupier who qualifies for a home loss payment is entitled to 10% of the market value of their interest in the property. In addition, the owner of the building can claim other reasonable costs associated with buying or renting another property (but not the price of the property or the rent itself) and reasonable costs of moving into and making changes to the new property [17]. Accordingly, the  $\mu$  in Eqs. (4) is set to 1.2 in this research.  $H_1$ ,  $S_{bottom}$ ,  $V$  in Eqs. (4) can be calculated automatically and are determined by geometric characteristics of a buildings' as-is BIM model. Thus  $C_{demolition}$  of each building's as-is BIM model can be determined by Eqs. (4). Using the DSM, DTM, and topography data, buildings' as-is BIM models can be built, and the data of height ( $H_1$ ), area ( $S_{bottom}$ ), volume ( $V$ ), and demolition costs ( $C_{demolition}$ ) of each building can be stored in the building's as-is BIM models using the proposed approach in Section 3.2, as shown in Fig. 18.

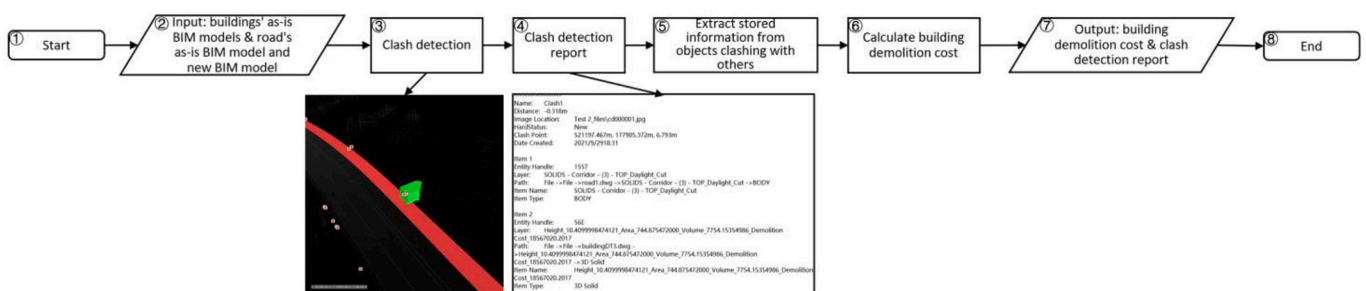


Fig. 14. Building demolition and costs estimation.



Fig. 15. Target research area.

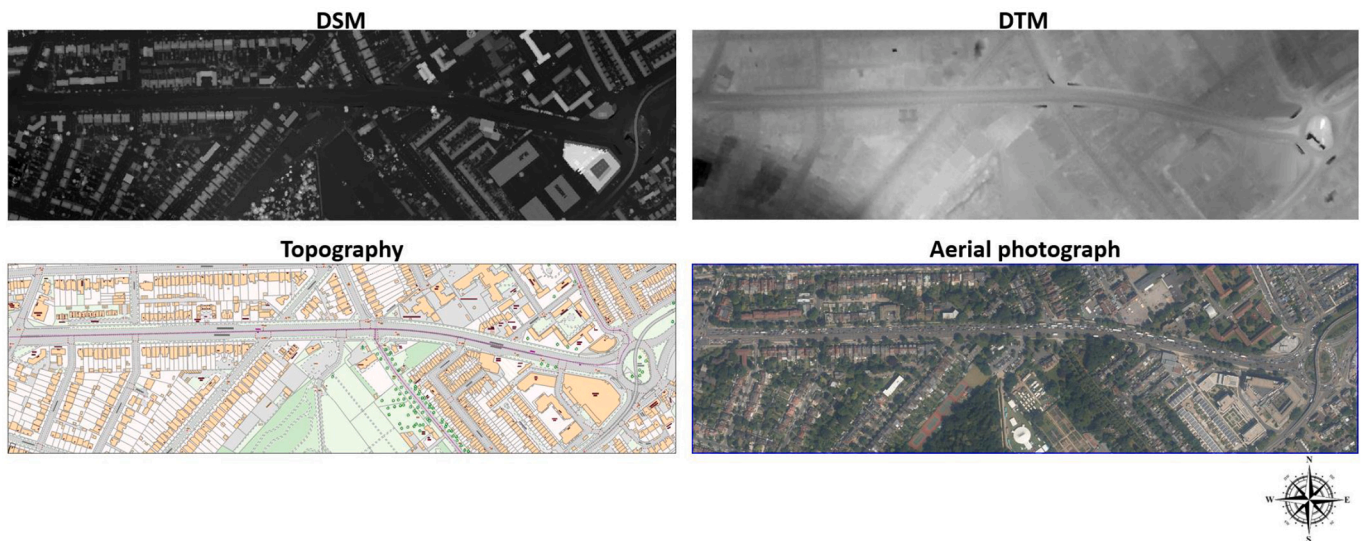


Fig. 16. Original map data.

$$P_{\text{upd}} = P_{\text{July 2021}} = \frac{12 \bullet P_{2016} \bullet P_{\text{July 2021}}}{\sum_{i=\text{January}}^{\text{December}} P_{i,2016}} \quad (16)$$

According to the proposed method in Section 3.1, on the pavement, there are four road markings lines that need to be fitted by smoothing splines 1–4 to create horizontal road marking lines, named HRML1, HRM2, HRM3, HRM4 from left to right, respectively. In addition to horizontal road marking lines, central horizontal alignment (CHA) needs to be fitted by smoothing splines and created. The results of HRMLs, CHA, and the parameters of their corresponding smoothing splines are shown in Table 2. The results are expressed by the stations and corresponding (x,y) coordinates, where x coordinates denote the West-East direction, and y coordinates denote the South-North direction.  $\lambda$ , RMSE, R-square of each corresponding smoothing spline are introduced in Eqs. (7) – Eqs. (11). The results of all the corresponding smoothing splines are shown in Fig. 19, and the result of HRMLs and CHA are shown in Fig. 20. Similarly, the results of the corresponding vertical road marking alignments (VRMLs) for HRMLs are shown in Table 3, where the results are expressed by the stations (S) and corresponding elevations (E). The parameters for Hampel filters n and t are introduced in Eqs. (12) – Eqs. (15), and  $\lambda$ , RMSE, R-square of each corresponding smoothing spline for VRMLs are introduced in Eqs. (7) – Eqs. (11). The results of elevations ( $E_1$ ) on the MDSM along the HRMLs, elevations ( $E_2$ ) after Hampel filter, the smoothing spline ( $E_3$ -S) for fitting, and the

VRMLs (E4-S) are shown in Fig. 21.

After fitting and creating the horizontal and vertical alignments, the cross-section assembly is established for the road's as-is BIM model and new road BIM model according to Section 3.1. All the constraints are shown in Table 4. The road's as-is BIM model for the existing old parts and road new BIM model for newly widened parts are established with information such as ModelType (as-is BIM model or BIM model), RoadComponent (central reserve, pavement, verge, or side slope), RoadPart (existing old part or widened part), Side (Right, Middle, or Left), Volume and other attributes, as shown in Fig. 22. The buildings' as-is BIM models are also established with information such as Height (m), Area ( $m^2$ ), Volume ( $m^3$ ), Demolition Cost (£), etc., as shown in Fig. 22. The road BIM models meet LoD 200, and the building BIM models meet LoD 100. After that, clash detection is conducted between the buildings' as-is BIM models and the road BIM models (as-is BIM models and new BIM models), as shown in Fig. 23. The clash detection report can be exported, as shown in Fig. 24, and the height, area, volume, and demolition costs of each building that clashes with the road's BIM models that need to be demolished can be extracted from the clash detection report, as shown in Table 5. There are forty buildings that need to be demolished, and the total estimated demolition areas, volumes, and costs are  $4216.365m^2$ ,  $31,962.789m^3$ , and  $76,533,660.03£$ , respectively.

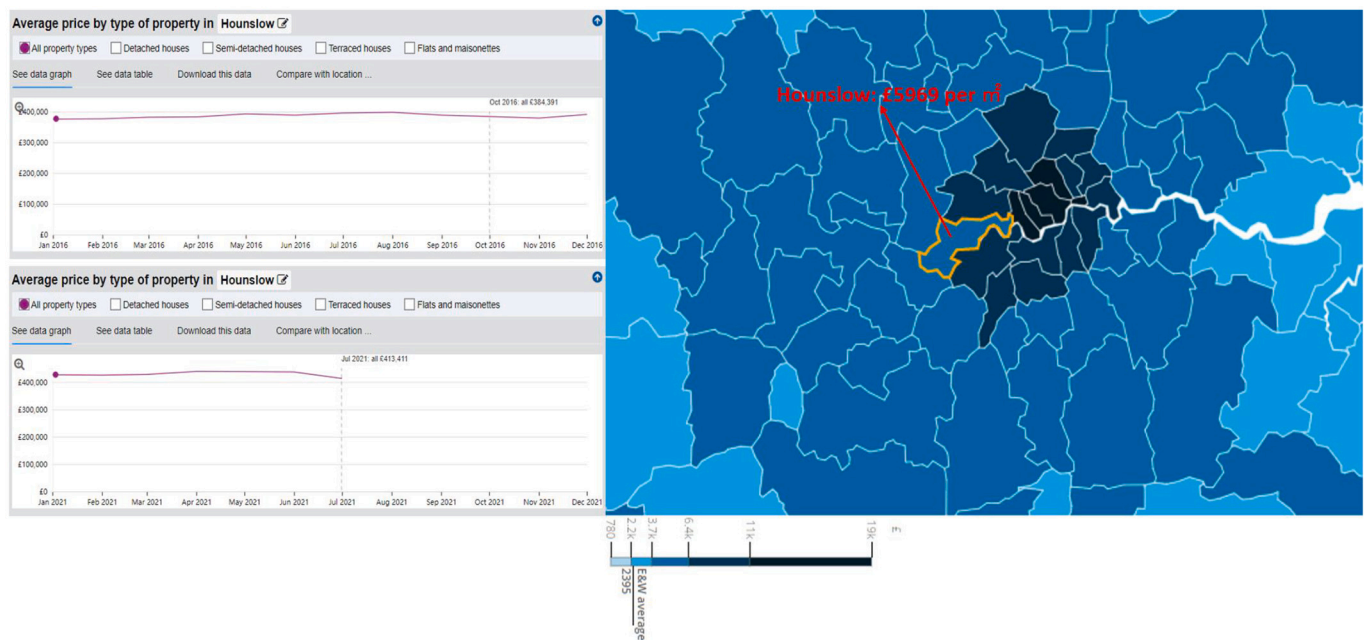


Fig. 17. House prices in the target research area.

Table 1  
House price data in the target research area.

Type	Average price of a property							
Time	Jan/2016	Feb/2016	Mar/2016	Apr/2016	May/2016	Jun/2016	Jul/2016	Aug/2016
Price	375,818 £	376,991 £	382,232 £	383,043 £	392,697 £	388,955 £	395,611 £	398,008 £
Type	Average price of a property					Average property price per m <sup>2</sup>		
Time	Sep/2016	Oct/2016	Nov/2016	Dec/2016	Jul/2021	2016	Jul/2021	
Price	388,796 £	384,391 £	379,542 £	391,460 £	413,411 £	5969 £/m <sup>2</sup>	6385.23 £/m <sup>2</sup>	

### 5. Discussion

This research focuses on urban road widening, a common way to improve roads' level of service, and building demolition, one of the most critical factors that restrict the road widening process. By leveraging the as-is BIM, this research can provide academics and designers with a systematic approach to estimate building demolition quantity and costs in urban road widening projects using online map data in the preliminary design phase with a field survey.

Compared with the two traditional methods, the proposed method is a compromise, as shown in the case study. One traditional method is to draw and offset the edge of the existing road on the 2D map to represent the new edge of the widened road to estimate the building demolition. The other traditional method is the field surveys and negotiations with the properties' owners. The former is a very rough estimation without considering 3D building models, 3D road models and road components. Thus, the positions of the toes of the side slopes cannot be predicted correctly. The latter is labour-intensive, costly, and time-consuming. At the preliminary design stage, detailed field surveys are unnecessary, and they are not convenient for the iteration of the design plan. In a compromise, the proposed method is cost-effective.

From the perspective of data collection, it is difficult to find the original design data and documents in the past of an old project and its surroundings. Even if some original data can be collected, they are often 2D paper drawings or PDF drawings. They are unstructured data that are difficult to be used for modelling and road widening. As-is BIM can provide a feasible solution to rebuild the existing old road and its surroundings to assist the design of the road widening. The proposed

method can build as-is BIM models for the existing old road and surrounding buildings based on downloaded online map data, policy, and government statistics. Based on the as-is BIM model of the existing old road, the BIM model of the newly widened road can be created.

From the perspective of different types of engineering, fewer studies employ as-is BIM models in long-shape alignment-based infrastructure, like roads, compared with buildings. In addition to BIM, GIS and surroundings also should be considered in road engineering. This research proposes a method to build as-is BIM models for roads considering road components (road alignment, central reserve, hard strip, lane, hard shoulder, verge, side slope, crossfall, and superelevation) in accordance with road engineering expressions from online map data. In addition, as-is BIM is an ideal paradigm for reconstructing existing old roads to assist in road widening. Generally, the road digitalisation should not only focus on a structure on one site, but also focus on the whole project along the road alignment and consider surroundings, environment, and GIS technology [19] road widening applications.

From the perspective of project phases, as-is BIM is implemented more in operation and maintenance phase in the civil engineering sector than in the design phase. In addition, many existing studies focus on how to build as-is BIM models rather than how to employ as-is BIM models in the design phase. As-is BIM models can be built for the existing environment, surroundings, and existing old projects to assist the design of a new project. Using as-is BIM models in the reconstruction and expansion projects based on the existing old projects and surroundings is very suitable, such as road widening projects. This research employs as-is BIM to assist building demolition estimation in the road widening projects in the preliminary design phase using as-is BIM.

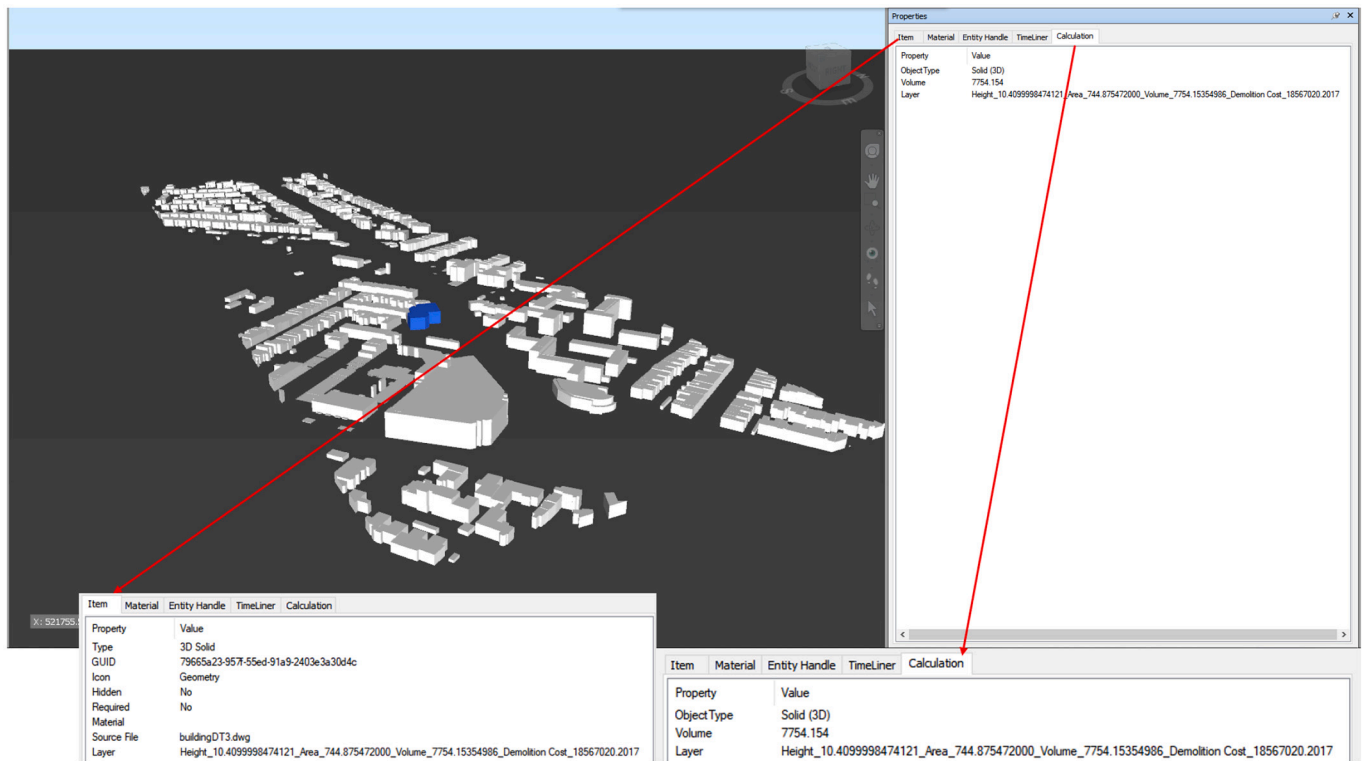


Fig. 18. Buildings' as-is BIM models.

Table 2  
Horizontal alignment fitting results.

HRML1			HRML2			HRML3		
Station	x	y	Station	x	y	Station	x	y
K0 + 000	520,554.0000	177,952.0102	K0 + 000	520,554.0720	177,948.9533	K0 + 000	520,554.2542	177,941.2132
K0 + 100	520,653.9709	177,954.4194	K0 + 100	520,654.0440	177,951.3175	K0 + 100	520,654.2274	177,943.5277
K0 + 200	520,753.9454	177,956.6773	K0 + 200	520,754.0209	177,953.4660	K0 + 200	520,754.2001	177,945.8676
K0 + 300	520,853.9178	177,959.0279	K0 + 300	520,853.9948	177,955.7507	K0 + 300	520,854.1725	177,948.2161
K0 + 400	520,953.8869	177,961.5113	K0 + 400	520,953.9608	177,958.3566	K0 + 400	520,954.1423	177,950.6674
K0 + 500	521,053.8283	177,960.1355	K0 + 500	521,053.9007	177,957.0243	K0 + 500	521,054.0859	177,949.3053
K0 + 600	521,152.7729	177,946.1097	K0 + 600	521,152.8421	177,942.9414	K0 + 600	521,152.9942	177,935.0791
K0 + 700	521,250.3674	177,924.3176	K0 + 700	521,250.4243	177,921.0930	K0 + 700	521,250.5868	177,913.2741
K0 + 735.495	521,285.0000	177,916.5402	K0 + 734.735	521,284.3173	177,913.4909	K0 + 732.868	521,282.6526	177,906.0553
$\lambda$	5.00E-06		$\lambda$	5.00E-06		$\lambda$	5.00E-06	
<b>RMSE</b>	0.1405		<b>RMSE</b>	0.1378		<b>RMSE</b>	0.1266	
<b>R-square</b>	0.9999		<b>R-square</b>	0.9999		<b>R-square</b>	0.9999	
HRML4			CHA					
Station	x	y	Station	x	y			
K0 + 000	520,554.3268	177,938.1308	K0 + 000	520,554.5817	177,945.0841			
K0 + 100	520,654.2984	177,940.5155	K0 + 100	520,654.5542	177,947.4278			
K0 + 200	520,754.2723	177,942.7989	K0 + 200	520,754.5289	177,949.6752			
K0 + 300	520,854.2445	177,945.1574	K0 + 300	520,854.5021	177,951.9919			
K0 + 400	520,954.2165	177,947.5236	K0 + 400	520,954.4692	177,954.5559			
K0 + 500	521,054.1600	177,946.0130	K0 + 500	521,054.4120	177,953.1171			
K0 + 600	521,153.0734	177,931.8230	K0 + 600	521,153.3274	177,938.8996			
K0 + 700	521,250.6617	177,909.9969	K0 + 700	521,250.9201	177,917.0981			
0 + 732.079	521,281.9662	177,902.9893	0 + 732.885	521,283.0000	177,909.8677			
$\lambda$	5.00E-06		$\lambda$	5.00E-06				
<b>RMSE</b>	0.1293		<b>RMSE</b>	3.8728				
<b>R-square</b>	0.9999		<b>R-square</b>	0.8947				

From the perspective of applications, in addition to building demolition quantity and costs estimation for a road-widening project in the case study, the proposed method also can estimate the building demolition quantity and costs for multiple potential roads that need to be widened in a city. Thus, it can assist in decision-making on which road is more suitable for priority to be widened [32]. Furthermore, one of the most important features is that the as-is BIM model of the existing old

road and the new BIM model of the newly widened road are detachable considering road components. Thus, according to the clash detection report, which component of the road has a clash with the buildings can be obtained. Therefore, if the clash is between the road's side slope with buildings rather than other road components with buildings in an area, retaining walls can be built to reduce the building demolition. Therefore, another derived potential application is to determine where

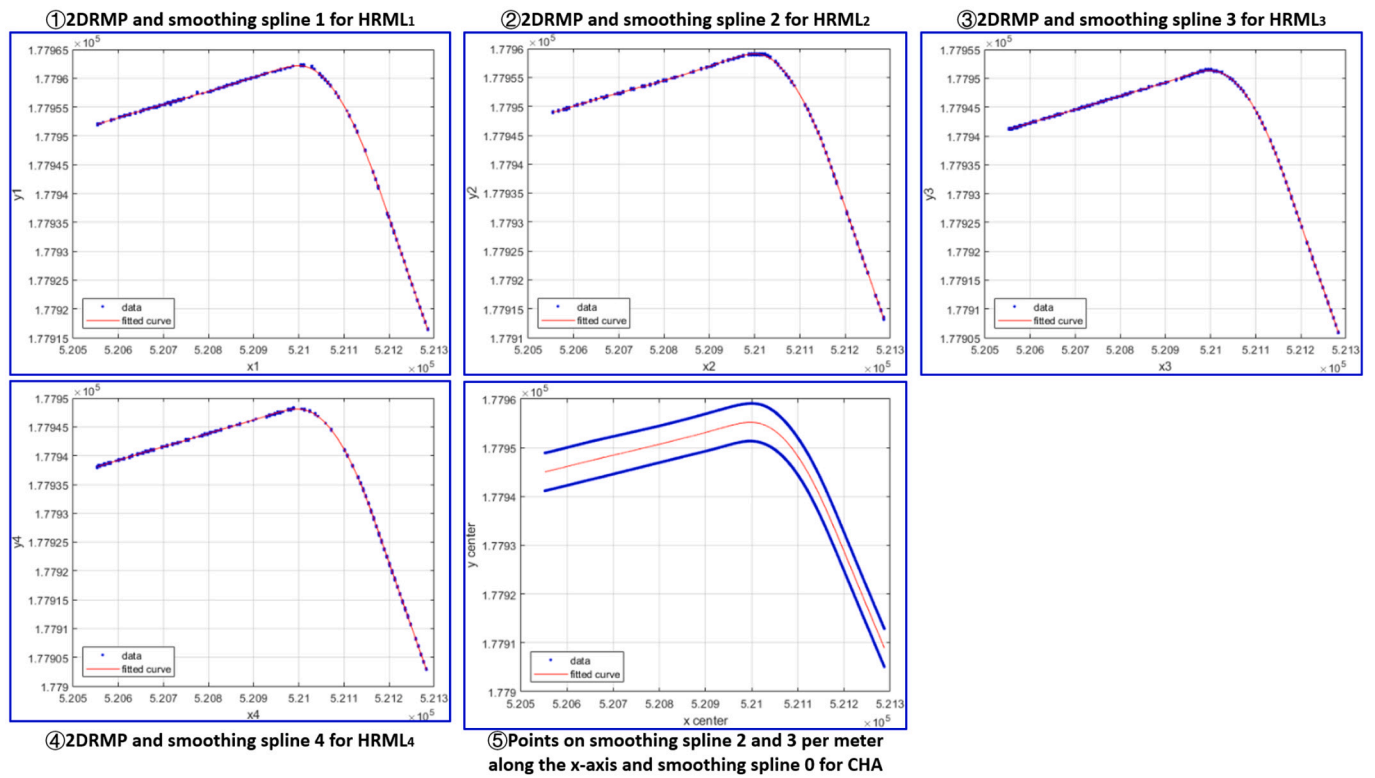


Fig. 19. Horizontal alignment fitting.



Fig. 20. Horizontal alignments.

Table 3  
Vertical alignment fitting results.

VRML1		VRML2		VRML3		VRML4	
Station	E	Station	E	Station	E	Station	E
K0 + 000	6.5300	K0 + 000	6.5703	K0 + 000	6.6135	K0 + 000	6.5444
K0 + 100	6.9814	K0 + 100	7.0705	K0 + 100	7.1834	K0 + 100	7.0908
K0 + 200	7.4129	K0 + 200	7.4959	K0 + 200	7.6368	K0 + 200	7.5560
K0 + 300	7.5273	K0 + 300	7.6175	K0 + 300	7.6583	K0 + 300	7.5912
K0 + 400	7.2620	K0 + 400	7.3102	K0 + 400	7.3166	K0 + 400	7.2311
K0 + 500	7.1422	K0 + 500	7.0379	K0 + 500	6.9704	K0 + 500	6.8429
K0 + 600	6.5813	K0 + 600	6.5080	K0 + 600	6.5667	K0 + 600	6.4472
K0 + 700	6.2352	K0 + 700	6.3106	K0 + 700	6.4724	K0 + 700	6.3700
K0 + 735	6.3669	K0 + 734	6.4277	K0 + 732	6.5672	K0 + 732	6.4458
n	700	n	700	n	700	n	700
t	0.1	t	0.1	t	0.1	t	0.1
$\lambda$	1.00E-07	$\lambda$	1.00E-07	$\lambda$	1.00E-07	$\lambda$	1.00E-07
RMSE	0.0248	RMSE	0.0202	RMSE	0.0194	RMSE	0.0224
R-square	0.9967	R-square	0.9980	R-square	0.9980	R-square	0.9975



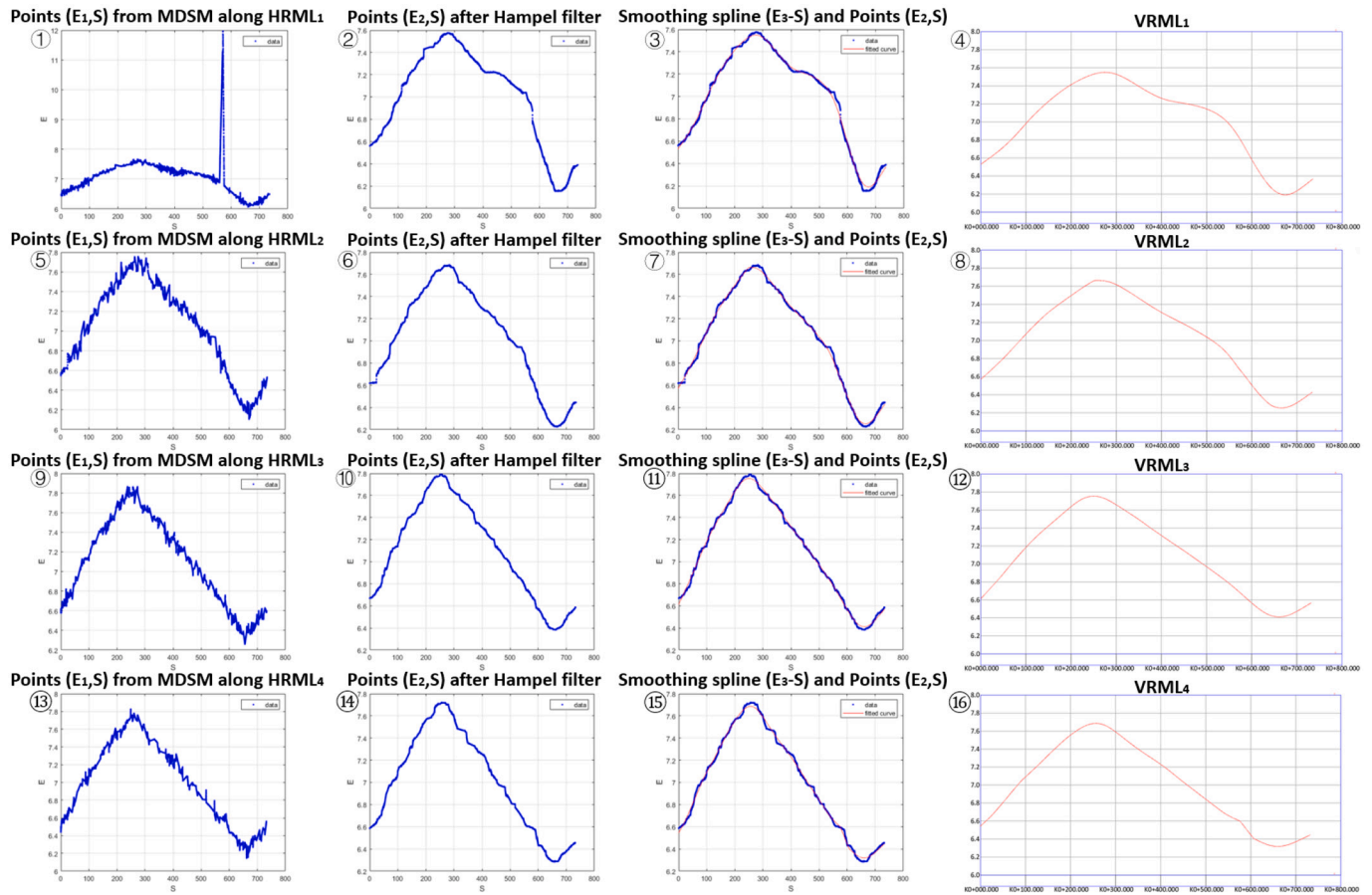


Fig. 21. Vertical alignment fitting.

Table 4  
Constraints for road's as-is BIM model and new BIM model.

Elements	Constraints	Elements	Constraints	Elements	Constraints
VL7	CHA	VL3	VL4&D2	P13	Extended L9∩VL13
VL4	HRML1	VL11	VL10&D2	L2	P2&P3
VL5	HRML2	VL2	VL7&D3	L3	P3&P4
VL9	HRML3	VL12	VL7&D3	L4	P4&P5
VL10	HRML4	VL1	VL2&D4	L6	P6&P7
P5	x = VL4, y = HL1	VL13	VL12&D4	L7	P7&P8
P6	x = VL5, y = HL2	L5	P5&P6	L8	P8&P9
P9	x = VL9, y = HL3	L9	P9&P10	L10	P10&P11
P10	x = VL10, y = HL4	P2	Extended L5∩VL1	L11	P11&P12
D1	1.05 m	P3	Extended L5∩VL2	L12	P12&P13
D2	3.1 m	P4	Extended L5∩VL3	Slope	33.33%
D3	19.2 m	P7	Extended L5∩VL6	L1	P2&Slope&terrain
D4	1.5 m	P8	Extended L9∩VL8	L2	P13&Slope&terrain
VL6	VL7&D1	P11	Extended L9∩VL11	P1	L1&terrain
VL8	VL7&D1	P12	Extended L9∩VL12	P14	L13&terrain

retaining walls should be built in a road widening project. We will consider these two potential applications in future research.

However, some limitations still exist in this research. First, due to the workload constraints, the field survey and negotiations with the properties' owners are not conducted with the proposed approach to evaluate its accuracy. Nevertheless, the proposed approach focuses on providing a low-cost workflow to estimate the building demolition quantity and costs caused by road widening at the preliminary design stage. Second, some roads have multi-level side slopes, but this research only considers the single-level side slope. Third, the research paradigm, such as design science research (DSR), should be employed, and exploratory and explanatory focus groups should be conducted to

evaluate and refine the proposed method iteratively.

## 6. Conclusions

Urban road widening is a common and effective way to improve existing old roads' level of service to meet current and future demands from society. Building demolition can cause economic, environmental, and democratic issues, which hinder the road widening process. Reconstruction and expansion projects such as road widening should be conducted based on the existing old projects, which are suitable for employing as-is BIM. This paper proposes a novel approach to build as-is BIM models for an existing old road and its surrounding buildings using

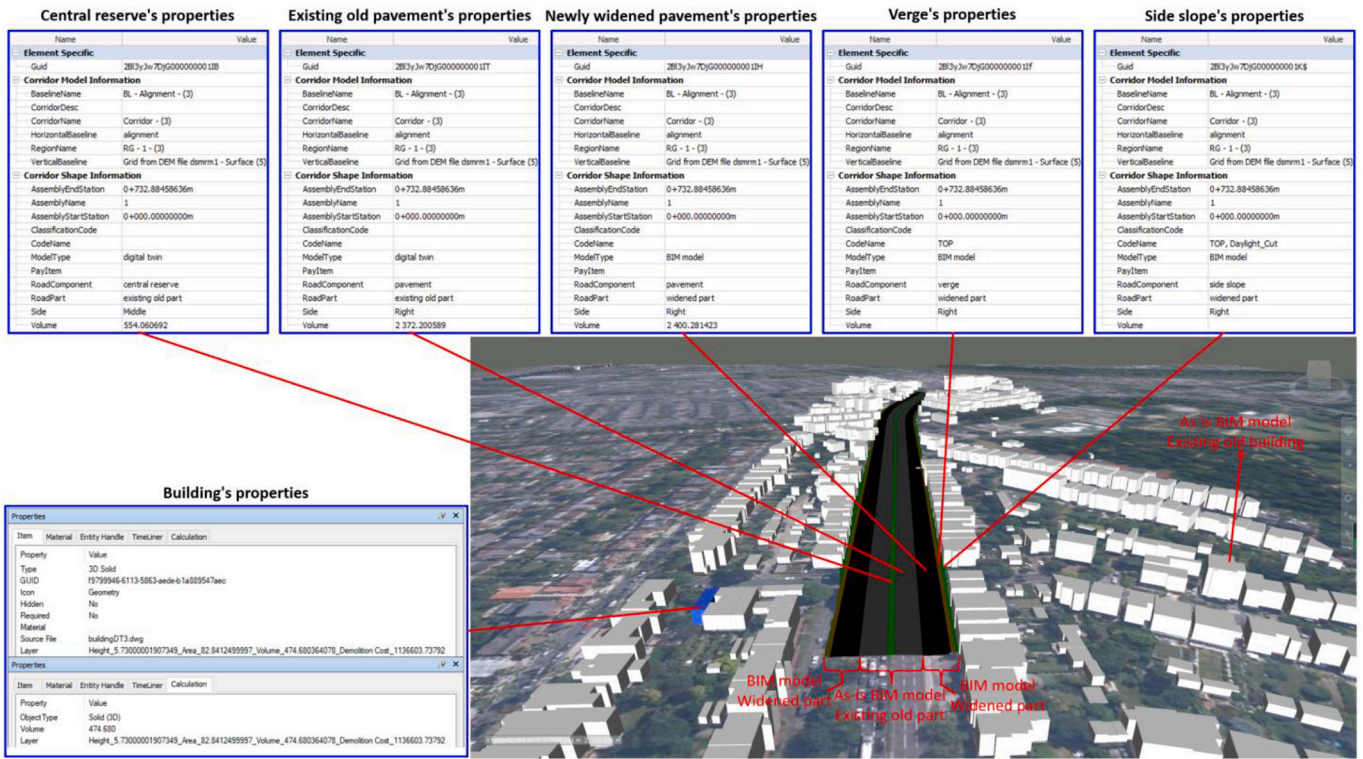


Fig. 22. Buildings' as-is BIM models, road's as-is BIM model, and new BIM model for the widened road.

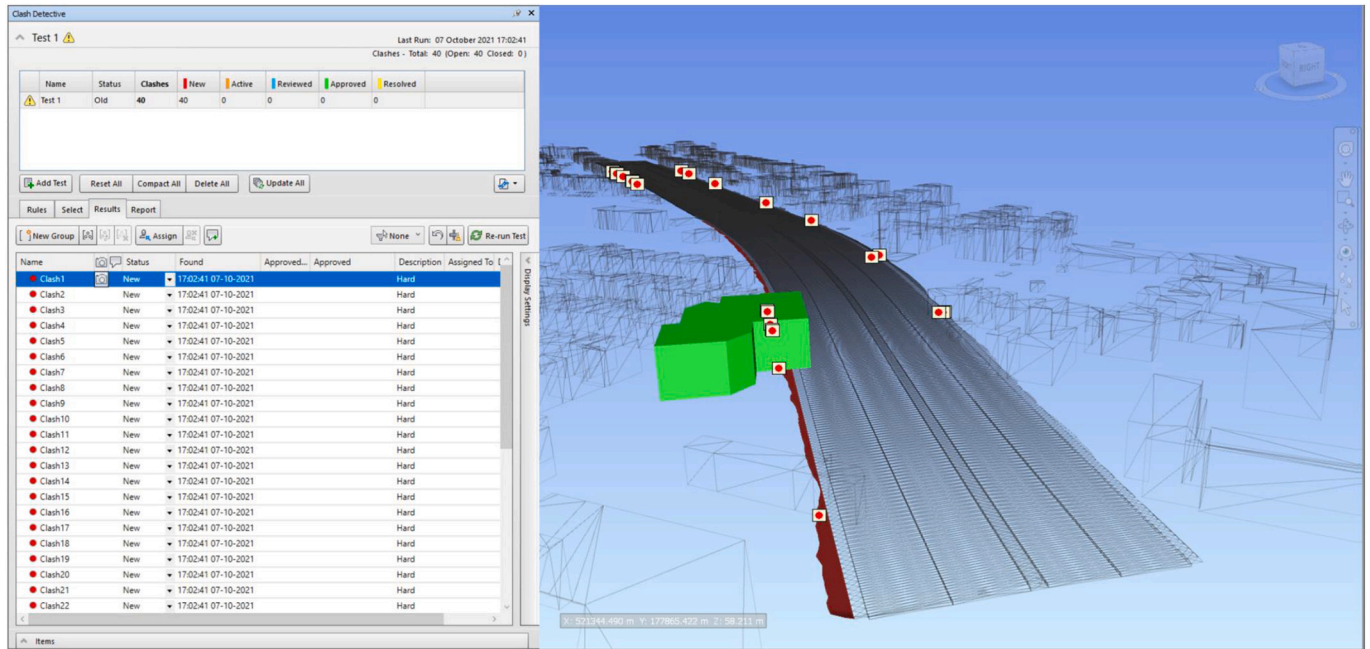


Fig. 23. Clash detection.

online map data without a field survey. Based on the road's as-is BIM model, new BIM models can be established for the newly widened road at the design stage. Useful information can be collected, analysed, calculated and stored as various attributes in the as-is BIM models and new BIM models. The road BIM models are detachable and consider road components in accordance with expressions in the field of road engineering. Then a clash detection can be conducted between the buildings' as-is BIM models and the road BIM models to estimate the potential

buildings' demolition quantity and costs caused by the road widening. There are several contributions that this article can bring to the field:

- 1) This paper develops a systematic workflow based on as-is BIM to estimate building demolition caused by urban road widening, which can assist urban road planning and decision making.
- 2) A systematic method is proposed to build as-is BIM models for roads in accordance with expressions of engineering by digital image



Fig. 24. Clash detection report and BIM models' information for building demolition costs estimation.

**Table 5**  
Building demolition caused by road widening.

No.	Height(m)	Area(m <sup>2</sup> )	Volume(m <sup>3</sup> )	Demolition Cost(£)	No.	Height(m)	Area(m <sup>2</sup> )	Volume(m <sup>3</sup> )	Demolition Cost(£)
1	10.410	744.875	7754.154	18,567,020.20	21	8.710	105.496	918.867	2,200,191.45
2	0.355	143.784	51.043	122,220.92	22	7.340	87.072	639.110	1,530,324.11
3	5.840	123.686	722.329	1,729,588.79	23	5.970	71.057	424.213	1,015,762.21
4	10.640	160.348	1706.097	4,085,183.88	24	6.990	99.819	697.737	1,670,704.05
5	0.355	143.784	51.043	122,220.92	25	6.810	68.261	464.859	1,113,087.20
6	6.730	107.224	721.620	1,727,891.67	26	6.380	131.524	839.126	2,009,253.89
7	7.250	81.490	590.802	1,414,653.38	27	8.440	87.958	742.361	1,777,555.48
8	6.640	97.273	645.895	1,546,571.31	28	7.525	93.438	703.117	1,683,586.88
9	6.640	97.273	645.895	1,546,571.31	29	7.050	127.724	900.453	2,156,098.96
10	7.840	100.978	791.664	1,895,607.79	30	9.200	33.958	312.409	748,051.15
11	6.640	97.273	645.895	1,546,571.31	31	9.280	75.579	701.371	1,679,406.44
12	6.005	54.251	325.775	780,055.42	32	5.795	19.626	113.734	272,331.94
13	8.256	105.722	872.839	2,089,979.27	33	10.400	176.548	1836.103	4,396,478.60
14	6.165	57.740	355.967	852,348.98	34	2.420	32.291	78.145	187,115.42
15	2.650	14.119	37.415	89,588.02	35	8.560	112.467	962.718	2,305,190.27
16	6.995	94.566	661.489	1,583,909.76	36	6.840	69.374	474.516	1,136,211.28
17	7.730	81.280	628.294	1,504,426.60	37	8.230	113.961	937.899	2,245,763.64
18	6.460	47.786	308.700	739,169.88	38	5.930	73.599	436.441	1,045,040.04
19	8.070	96.192	776.271	1,858,750.40	39	9.170	34.610	317.374	759,939.03
20	5.730	60.280	345.403	827,053.56	40	8.945	92.079	823.644	1,972,184.58
				<b>Total:</b>			<b>4216.365</b>	<b>31,962.789</b>	<b>76,533,660.03</b>

- processing, GIS data processing, alignment fitting, and cross-section fitting.
- 3) A method is proposed to create as-is BIM models of the buildings along the target road, which can reflect the impacts of the surrounding built environment on existing infrastructure.

- 4) Several methods are proposed to build BIM models for roads and buildings from online map data and government statistics rather than field surveys.

However, this paper has some limitations that should be addressed in future research. First of all, the accuracy of the proposed method is only

estimated by simple quantitative methods and has not been systematically estimated by both qualitative and quantitative methods. Thus, in future research, A detailed field survey should be conducted to evaluate the proposed approach as a quantitative method. Based on the design science research (DSR) paradigm, exploratory and explanatory focus groups should be conducted to evaluate and refine the proposed method iteratively as a qualitative analysis. Moreover, the road is selected in a plain area in the city, and the road BIM models only consider single-level side slopes. Thus, multi-level side slopes on the hilly terrain should be considered in future research. In addition to the research limitations, further and interesting studies can be conducted based on this paper as extensions. First, building demolition quantity and costs of multiple roads in the road network should be estimated to assist in decision-making on which road is more suitable for priority to be widened in a city. Second, where to build retaining walls in a road widening project can be studied based on the proposed method.

### Declaration of Competing Interest

The authors declare that they have no known competing financial interests or personal relationships that could have appeared to influence the work reported in this paper.

### Data availability

No data was used for the research described in the article.

### Acknowledgement

This study is supported by Major Science & Technology Project of Hubei (Grant No. 2020ACA006).

### References

- [1] R. Abdelmaksoud, S. Abdellatif, A. Aboulela, M. El Tawil, O. Rizk, A. Sefein, O. El Kadi, M.N. Abouzeid, S. Khedr, E.Y. Sayed-Ahmed, Rehabilitation of a historic building in Egypt: King farouk rest house, in: A. Zingoni (Ed.), 7th International Conference on Structural Engineering, Mechanics and Computation, 2019, CRC Press, Balkema, 2019, pp. 2170–2175, <https://doi.org/10.1201/9780429426506-374>.
- [2] A. Adán, B. Quintana, S.A. Prieto, F. Bosché, Scan-to-BIM for 'secondary' building components, *Adv. Eng. Inform.* 37 (2018) 119–138, <https://doi.org/10.1016/j.aei.2018.05.001>.
- [3] G.A. Adeyemi, O.G. Gbolahan, M. Markus, S.O. Edeki, Geospatial analysis of building demolition during road expansion project in Ado-Odo OTA settings, *Int. J. Civ. Eng. Technol.* 9 (12) (2018) 303–314, [https://iaeme.com/Home/article\\_id/IJCIET\\_09\\_12\\_034](https://iaeme.com/Home/article_id/IJCIET_09_12_034).
- [4] J.Á. Aranda, M.M. Santonja, M.Á.G. Sauri, G. Peris-Fajarnés, Minimizing shadow area in mountain roads for improving the sustainability of infrastructures, *Sustainability (Switzerland)* 13 (10) (2021), <https://doi.org/10.3390/su13105392>.
- [5] S. Azhar, Building information modeling (BIM): trends, benefits, risks, and challenges for the AEC industry, *Leadersh. Manag. Eng.* 11 (3) (2011) 241–252, [https://doi.org/10.1061/\(ASCE\)LM.1943-5630.0000127](https://doi.org/10.1061/(ASCE)LM.1943-5630.0000127).
- [6] L. Barazzetti, M. Previtali, M. Scaioni, Roads detection and parametrization in integrated BIM-GIS using LiDAR, *Infrastructures* 5 (7) (2020), <https://doi.org/10.3390/infrastructures5070055>.
- [7] S.A. Biancardo, A. Capano, S.G. de Oliveira, A. Tibaut, Integration of BIM and procedural modeling tools for road design, *Infrastructures* 5 (4) (2020), <https://doi.org/10.3390/infrastructures5040037>.
- [8] N. Bongiorno, G. Bosurgi, F. Carbone, O. Pellegrino, G. Sollazzo, Potentialities of a highway alignment optimization method in an i-bim environment, *Period. Polytech. Civ. Eng.* 63 (2) (2019) 352–361, <https://doi.org/10.3311/PPci.12220>.
- [9] G. Bosurgi, O. Pellegrino, G. Sollazzo, Pavement condition information modelling in an I-BIM environment, *Int. J. Pav. Eng.* (2021), <https://doi.org/10.1080/10298436.2021.1978442>.
- [10] S.P. Boyle, J.D. Litzgus, D. Lesbarrères, Limited evidence for negative effects of highway widening on North American large mammals, *Eur. J. Wildl. Res.* 66 (6) (2020), <https://doi.org/10.1007/s10344-020-01428-4>.
- [11] K. Castañeda, O. Sánchez, R.F. Herrera, E. Pellicer, H. Porras, BIM-based traffic analysis and simulation at road intersection design, *Autom. Constr.* 131 (2021), <https://doi.org/10.1016/j.autcon.2021.103911>.
- [12] L. Chen, Q. Lu, X. Zhao, A semi-automatic image-based object recognition system for constructing as-is IFC BIM objects based on fuzzy-MAUT, *Int. J. Constr. Manag.* 22 (1) (2022) 51–65, <https://doi.org/10.1080/15623599.2019.1615754>.
- [13] M. Chen, E. Koc, Z. Shi, L. Soibelman, Proactive 2D model-based scan planning for existing buildings, *Autom. Constr.* 93 (2018) 165–177, <https://doi.org/10.1016/j.autcon.2018.05.010>.
- [14] Y.J. Cheng, W.G. Qiu, D.Y. Duan, Automatic creation of as-is building information model from single-track railway tunnel point clouds, *Autom. Constr.* 106 (2019), <https://doi.org/10.1016/j.autcon.2019.102911>.
- [15] N. Concha, A.N. Cana, R. Mae Suzara, U. Fallarcuna, An artificial neural system to predict building demolition cost, in: 11th IEEE International Conference on Humanoid, Nanotechnology, Information Technology, Communication and Control, Environment, and Management, Institute of Electrical and Electronics Engineers Inc, 2019, <https://doi.org/10.1109/HNICEM48295.2019.9072750>.
- [16] Y. Deng, J.C.P. Cheng, C. Anumba, Mapping between BIM and 3D GIS in different levels of detail using schema mediation and instance comparison, *Autom. Constr.* 67 (2016) 1–21, <https://doi.org/10.1016/j.autcon.2016.03.006>.
- [17] Department for Levelling Up, Housing and Communities, Compulsory Purchase and Compensation Booklet 4: Compensation to Residential Owners and Purchasers, Retrieved from: [https://assets.publishing.service.gov.uk/government/uploads/system/uploads/attachment\\_data/file/571453/booklet4.pdf](https://assets.publishing.service.gov.uk/government/uploads/system/uploads/attachment_data/file/571453/booklet4.pdf), 2021 (Accessed date: 14 August 2022).
- [18] Digimap, Retrieved from, <https://digimap.edina.ac.uk/lidar>, 2022 (Accessed date: 14 August 2022).
- [19] M. Francini, S. Gaudio, A. Palermo, M.F. Viapiana, A performance-based approach for innovative emergency planning, *Sustain. Cities Soc.* 53 (2020), <https://doi.org/10.1016/j.scs.2019.101906>.
- [20] G. Gröger, L. Plümer, CityGML - interoperable semantic 3D city models, *ISPRS J. Photogramm. Remote Sens.* 71 (2012) 12–33, <https://doi.org/10.1016/j.isprsjprs.2012.04.004>.
- [21] HM Land Registry Open Data, UK House Price Index, Retrieved from: <https://landregistry.data.gov.uk/app/ukhpi/browse?from=2020-04-01&location=http%3A%2F%2Flandregistry.data.gov.uk%2Ffid%2Fregion%2Fhounslow&to=2021-04-01&lang=en>, 2021 (Accessed date: 14 August 2022).
- [22] A. Holgado-Barco, B. Riveiro, D. González-Aguilera, P. Arias, Automatic inventory of road cross-sections from mobile laser scanning system, *Comput. Aid. Civ. Infrastruct. Eng.* 32 (1) (2017) 3–17, <https://doi.org/10.1111/mice.12213>.
- [23] A. Husain, R.C. Vaishya, An AHP based automated approach for pole-like objects detection using three dimensional terrestrial laser scanner data, in: P. Bhattacharyya, H.G. Sastry, V. Marriboyina, R. Sharma (Eds.), 3rd International Conference on Next Generation Computing Technologies, NGCT 2017 vol. 828, Springer Verlag, 2018, pp. 692–703, [https://doi.org/10.1007/978-981-10-8660-1\\_52](https://doi.org/10.1007/978-981-10-8660-1_52).
- [24] International Organization for Standardization, ISO 19650-1, 2018—Organization and Digitization of Information About Buildings and Civil Engineering Works, Including Building Information Modelling (BIM)—Information Management Using Building Information Modelling. Part 1: Concepts and Principles, Retrieved from, <https://www.iso.org/standard/68078.html>, 2018 (Accessed date: 14 August 2022).
- [25] F. Jiang, L. Ma, T. Broyd, K. Chen, Digital twin and its implementations in the civil engineering sector, *Autom. Constr.* 130 (2021), <https://doi.org/10.1016/j.autcon.2021.103838>.
- [26] F. Jiang, L. Ma, T. Broyd, K. Chen, H. Luo, Underpass clearance checking in highway widening projects using digital twins, *Autom. Constr.* 141 (2022), <https://doi.org/10.1016/j.autcon.2022.104406>.
- [27] F. Jiang, L. Ma, T. Broyd, W. Chen, H. Luo, Building digital twins of existing highways using map data based on engineering expertise, *Autom. Constr.* 134 (2022), <https://doi.org/10.1016/j.autcon.2021.104081>.
- [28] F. Jiang, L. Ma, T. Broyd, W. Chen, H. Luo, Digital twin enabled sustainable urban road planning, *Sustain. Cities Soc.* 78 (2022), <https://doi.org/10.1016/j.scs.2021.103645>.
- [29] F. Jiménez, F. Aparicio, G. Estrada, Measurement uncertainty determination and curve-fitting algorithms for development of accurate digital maps for advanced driver assistance systems, *Transp. Res. Part C Emerg. Technol.* 17 (3) (2009) 225–239, <https://doi.org/10.1016/j.trc.2008.10.004>.
- [30] R. Jino, R. Murugasan, Assessment of highway widening and its dynamic interactions with land use pattern, *Ecol. Environ. Conserv.* 23 (September) (2017) S139–S145, [http://www.envirobiotechjournals.com/article\\_abstract.php?aid=8067&iid=233&jid=3](http://www.envirobiotechjournals.com/article_abstract.php?aid=8067&iid=233&jid=3).
- [31] A. Justo, M. Soilán, A. Sánchez-Rodríguez, B. Riveiro, Scan-to-BIM for the infrastructure domain: generation of IFC-complaint models of road infrastructure assets and semantics using 3D point cloud data, *Autom. Constr.* 127 (2021), <https://doi.org/10.1016/j.autcon.2021.103703>.
- [32] R. Khayamim, S.N. Shetab-Boushehri, S.M. Hosseiniinasab, H. Karimi, A sustainable approach for selecting and timing the urban transportation infrastructure projects in large-scale networks: a case study of Isfahan, Iran, *Sustain. Cities Soc.* 53 (2020), <https://doi.org/10.1016/j.scs.2019.101981>.
- [33] H. Kim, K. Orr, Z. Shen, H. Moon, K. Ju, W. Choi, Highway alignment construction comparison using object-oriented 3D visualization modeling, *J. Constr. Eng. Manag.* 140 (10) (2014), [https://doi.org/10.1061/\(ASCE\)CO.1943-7862.0000898](https://doi.org/10.1061/(ASCE)CO.1943-7862.0000898).
- [34] S.B. Lee, M. Song, S. Kim, J.H. Won, Change monitoring at expressway infrastructure construction sites using drone, *Sensors Mater.* 32 (11) (2020) 3923–3933, <https://doi.org/10.18494/SAM.2020.2971>.
- [35] S.S. Lee, K.T. Kim, W.A. Tanoli, J.W. Seo, Flexible 3D model partitioning system for nD-based BIM implementation of alignment-based civil infrastructure, *J. Manag. Eng.* 36 (1) (2020), [https://doi.org/10.1061/\(ASCE\)ME.1943-5479.0000725](https://doi.org/10.1061/(ASCE)ME.1943-5479.0000725).
- [36] LiDAR Digimap Help, Retrieved from: [https://digimap.edina.ac.uk/webhelp/lidar/lidarDigimaphelp.htm#copyright/licence\\_agreement.htm](https://digimap.edina.ac.uk/webhelp/lidar/lidarDigimaphelp.htm#copyright/licence_agreement.htm), 2022 (Accessed date: 14 August 2022).

- [37] S. Ling, S.F. Ma, N. Jia, Sustainable urban transportation development in China: a behavioral perspective, *Front. Eng. Manag.* 9 (1) (2022) 16–30, <https://doi.org/10.1007/s42524-021-0162-4>.
- [38] Q. Lu, L. Chen, S. Li, M. Pitt, Semi-automatic geometric digital twinning for existing buildings based on images and CAD drawings, *Autom. Constr.* 115 (2020), <https://doi.org/10.1016/j.autcon.2020.103183>.
- [39] Q. Lu, S. Lee, L. Chen, Image-driven fuzzy-based system to construct as-is IFC BIM objects, *Autom. Constr.* 92 (2018) 68–87, <https://doi.org/10.1016/j.autcon.2018.03.034>.
- [40] R. Lu, I. Brilakis, Digital twinning of existing reinforced concrete bridges from labelled point clusters, *Autom. Constr.* 105 (2019), <https://doi.org/10.1016/j.autcon.2019.102837>.
- [41] O.I. Maksimychev, M.Y. Karelina, A.V. Ostroukh, S.V. Zhankaziev, D.A. Pastukhov, Y.E.O. Nuruev, Automated control system of road construction works, *Int. J. Appl. Eng. Res.* 11 (9) (2016) 6441–6446, <https://www.semanticscholar.org/paper/Automated-Control-System-of-Road-Construction-Works-Maksimychev-Karelina/9c6996670bd96b1bc4b934a4e406526b59642b8c>.
- [42] M. Marzouk, M. El-zayat, A. Aboushady, Assessing environmental impact indicators in road construction projects in developing countries, *Sustainability (Switzerland)* 9 (5) (2017), <https://doi.org/10.3390/su9050843>.
- [43] Office for National Statistics, House Prices: How much Does One Square Metre Cost in your Area?, Retrieved from: <https://www.ons.gov.uk/peoplepopulationandcommunity/housing/articles/housepriceshowmuchdoesonesquaremetrecostinyourarea/2017-10-11>, 2017 (Accessed date: 14 August 2022).
- [44] Old Oak and Park Royal Development Corporation, Tall Buildings Statement, Retrieved from: [https://www.london.gov.uk/sites/default/files/52\\_tall\\_buildings\\_statement\\_2018.pdf](https://www.london.gov.uk/sites/default/files/52_tall_buildings_statement_2018.pdf), 2018 (Accessed date: 14 August 2022).
- [45] C. Oretto, S.A. Biancardo, N. Viscione, R. Veropalumbo, F. Russo, Road pavement information modeling through maintenance scenario evaluation, *J. Adv. Transp.* 2021 (2021), <https://doi.org/10.1155/2021/8823117>.
- [46] V.S. Phogat, A. Singhal, R.K. Mittal, A.P. Singh, The impact of construction of hill roads on the environment, assessed using the multi-criteria approach, *Int. J. Environ. Stud.* 79 (1) (2022) 1–18, <https://doi.org/10.1080/00207233.2021.1905298>.
- [47] M. Pyngrope, N. Hossiney, Y. Chen, H.K. Thejas, C.K. Sarath, J. Alex, S. Lakshmi Kumar, Properties of alkali-activated concrete (AAC) incorporating demolished building waste (DBW) as aggregates, *Cogent Eng.* 8 (1) (2021), <https://doi.org/10.1080/23311916.2020.1870791>.
- [48] Q. Qiu, M. Wang, J. Guo, Z. Liu, Q. Wang, An adaptive down-sampling method of laser scan data for scan-to-BIM, *Autom. Constr.* 135 (2022), <https://doi.org/10.1016/j.autcon.2022.104135>.
- [49] Q. Qiu, M. Wang, X. Tang, Q. Wang, Scan planning for existing buildings without BIM based on user-defined data quality requirements and genetic algorithm, *Autom. Constr.* 130 (2021), <https://doi.org/10.1016/j.autcon.2021.103841>.
- [50] E. Shahat, C.T. Hyun, C. Yeom, City digital twin potentials: a review and research agenda, *Sustainability (Switzerland)* 13 (6) (2021), <https://doi.org/10.3390/su13063386>.
- [51] Z. Shi, K. Lv, Green highway evaluation based on big Data GIS and BIM technology, *Arab. J. Geosci.* 14 (11) (2021), <https://doi.org/10.1007/s12517-021-07253-6>.
- [52] M. Soillán, A. Justo, A. Sánchez-Rodríguez, B. Riveiro, 3D point cloud to BIM: semi-automated framework to define IFC alignment entities from MLS-acquired LIDAR data of highway roads, *Remote Sens.* 12 (14) (2020), <https://doi.org/10.3390/rs12142301>.
- [53] W.J.V.D.M. Steyn, A. Broekman, Development of a digital twin of a local road network: a case study, *J. Test. Eval.* 51 (1) (2021), <https://doi.org/10.1520/JTE202100.43>.
- [54] C. Sun, W. Zhang, Y. Luo, J. Li, Road construction and air quality: empirical study of cities in China, *J. Clean. Prod.* 319 (2021), <https://doi.org/10.1016/j.jclepro.2021.128649>.
- [55] F. Tang, T. Ma, Y. Guan, Z. Zhang, Parametric modeling and structure verification of asphalt pavement based on BIM-ABAQUS, *Autom. Constr.* 111 (2020), <https://doi.org/10.1016/j.autcon.2019.103066>.
- [56] F. Tang, T. Ma, J. Zhang, Y. Guan, L. Chen, Integrating three-dimensional road design and pavement structure analysis based on BIM, *Autom. Constr.* 113 (2020), <https://doi.org/10.1016/j.autcon.2020.103152>.
- [57] E. Valero, A. Adan, C. Cerrada, Automatic construction of 3D basic-semantic models of inhabited interiors using laser scanners and RFID sensors, *Sensors (Switzerland)* 12 (5) (2012) 5705–5724, <https://doi.org/10.3390/s120505705>.
- [58] V. Vignali, E.M. Acerra, C. Lantieri, F. Di Vincenzo, G. Piacentini, S. Pancaldi, Building information modelling (BIM) application for an existing road infrastructure, *Autom. Constr.* 128 (2021), <https://doi.org/10.1016/j.autcon.2021.103752>.
- [59] C. Wang, Y.K. Cho, C. Kim, Automatic BIM component extraction from point clouds of existing buildings for sustainability applications, *Autom. Constr.* 56 (2015) 1–13, <https://doi.org/10.1016/j.autcon.2015.04.001>.
- [60] Q. Wang, J. Guo, M.K. Kim, An application oriented scan-to-bim framework, *Remote Sens.* 11 (3) (2019), <https://doi.org/10.3390/rs11030365>.
- [61] M.T. Wildenthal, J.L. Buffington, J.L. Memmott, Application of a user cost model to measure during and after construction costs and benefits: highway widening projects, *Transp. Res. Rec.* 1450 (1994) 38–43, <https://onlinepubs.trb.org/Onlinepubs/trr/1994/1450/1450-006.pdf>.
- [62] G. Yu, Y. Wang, M. Hu, L. Shi, Z. Mao, V. Sugumaran, RIOMS: an intelligent system for operation and maintenance of urban roads using spatio-temporal data in smart cities, *Futur. Gener. Comput. Syst.* 115 (2021) 583–609, <https://doi.org/10.1016/j.future.2020.09.010>.
- [63] G.W. Zeng, Z.Y. Sun, S.Y. Liu, X.Q. Chen, D.Q. Li, J.J. Wu, Z.Y. Gao, Percolation-based health management of complex traffic systems, *Front. Eng. Manag.* 8 (4) (2021) 557–571, <https://doi.org/10.1007/s42524-021-0174-0>.
- [64] L. Zhao, Z. Liu, J. Mbachu, Highway alignment optimization: an integrated BIM and GIS approach, *ISPRS Int. J. Geo Inf.* 8 (4) (2019), <https://doi.org/10.3390/ijgi8040172>.